Insights from 3D Simulations, Remote Imaging, and PSP Data on the Location and Dynamics of the Corrugated Alfven Zone

Rohit Chhiber

University of Delaware & NASA Goddard Space Flight Center

Collaborators: William Matthaeus, Arcadi Usmanov, Melvyn Goldstein

PUNCH 2 Science Meeting

10th August 2021

Outline

- Review work based on 3D sims – large-scale variability; solar activity effects
- Review recent observations that suggest a "rugged/corrugated" surface
- 3D simulations with turbulence modeling – turbulence effects on variability of Alfven zone
- Discussion and summary

3D MHD simulations of global solar wind

r_A is distance where $U > V_A$, where $V_A = \frac{B}{\sqrt{4\pi\rho}}$

Large-scale variability – solar-source related; solar activity effects

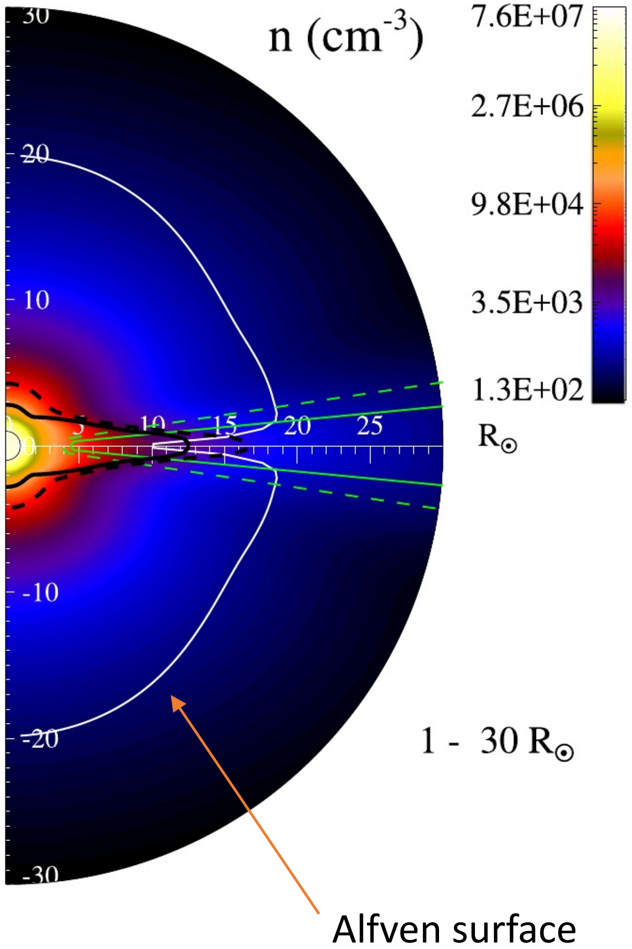

Untilted dipole; Chhiber+ 2019

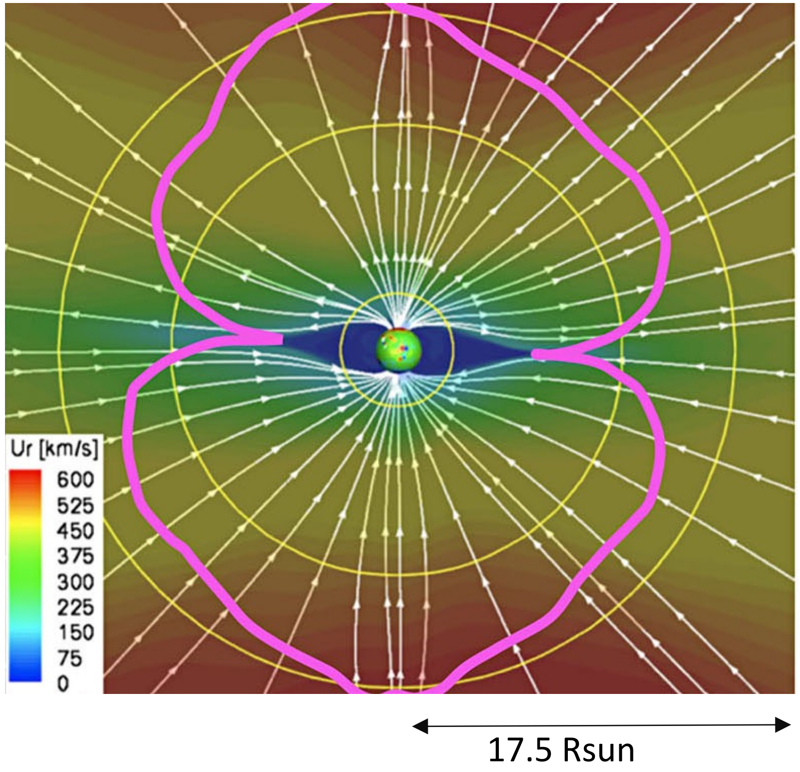

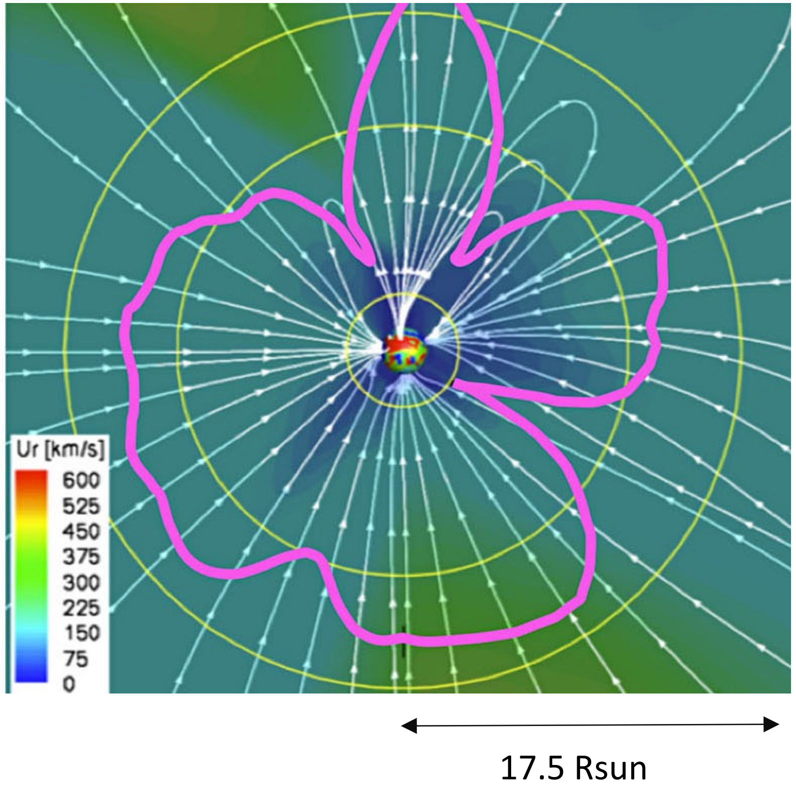

Solar min/max magnetograms; Cohen 2015; PUNCH website

3D MHD simulations of global solar wind – solar activity and Alfven surface

Increased complexity of magnetic topology brings Alfven surface lower

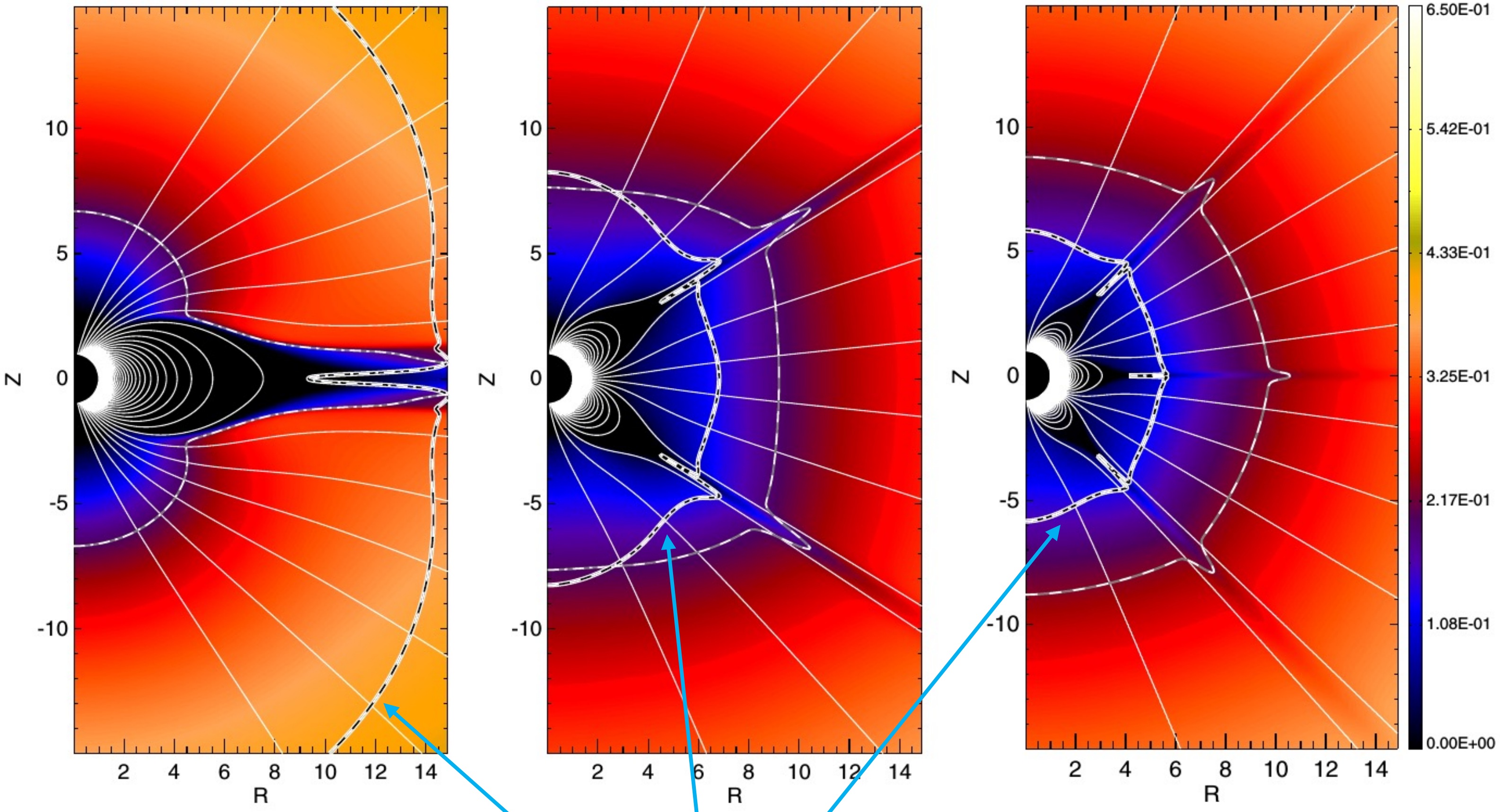

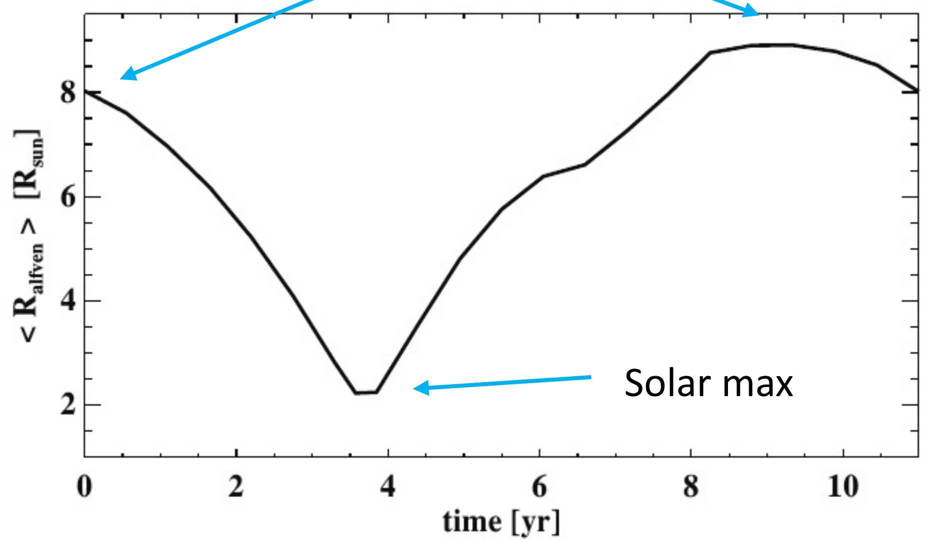

Pinto+ 2011 used solar dynamo model

Reville+ 2015

Alfven surface

Also seen in Pinto+ 2017; Perri+ 2018; Chhiber+ 2019

Observations - solar activity and Alfven surface

- Alfven radius appears correlated with sunspot number
- Caveat – 1 AU measurements; assumed radial scalings for B and n; constant speed

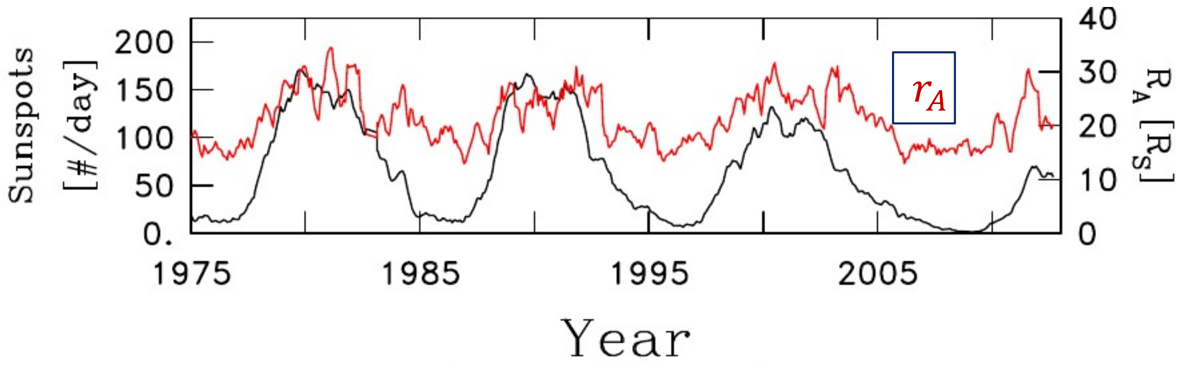

Top: Goelzer+ 2014

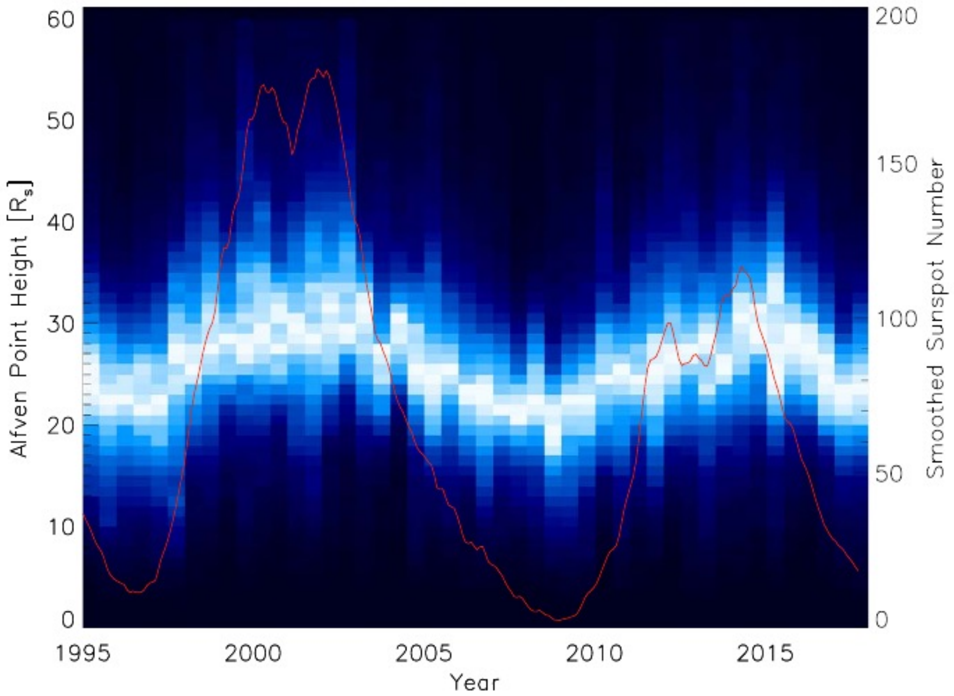

Kasper+ 2019

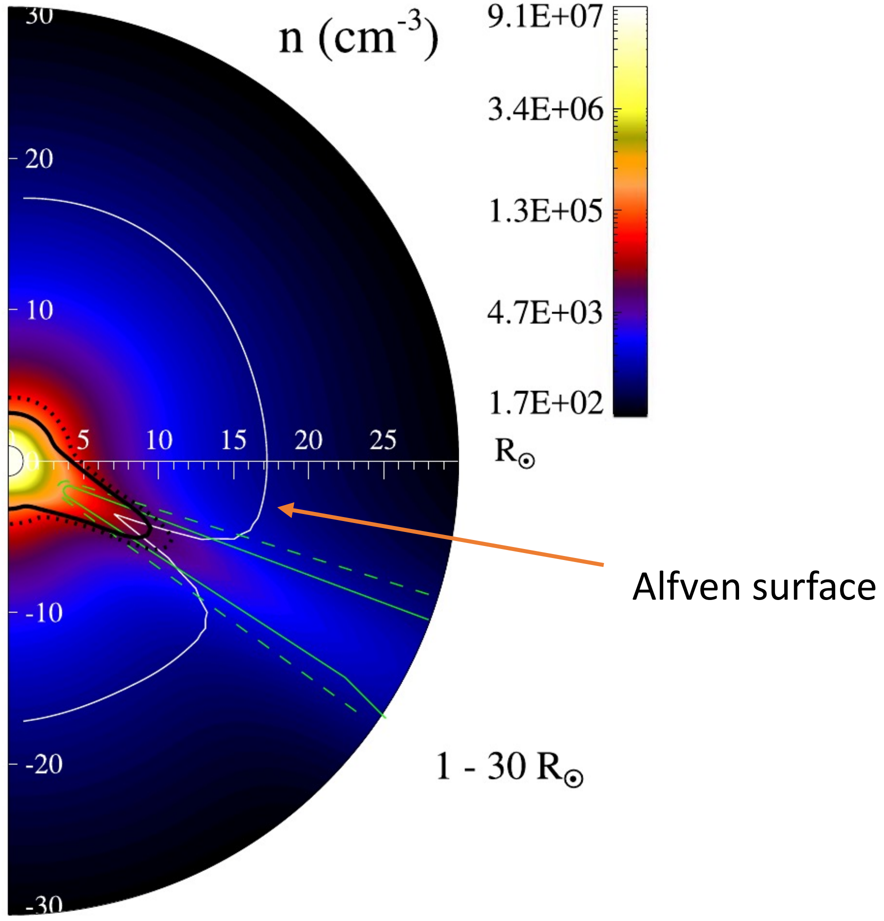

30 deg dipole tilt
Chhiber+ 2019

Corrugated Alfven surface - remote sensing observations

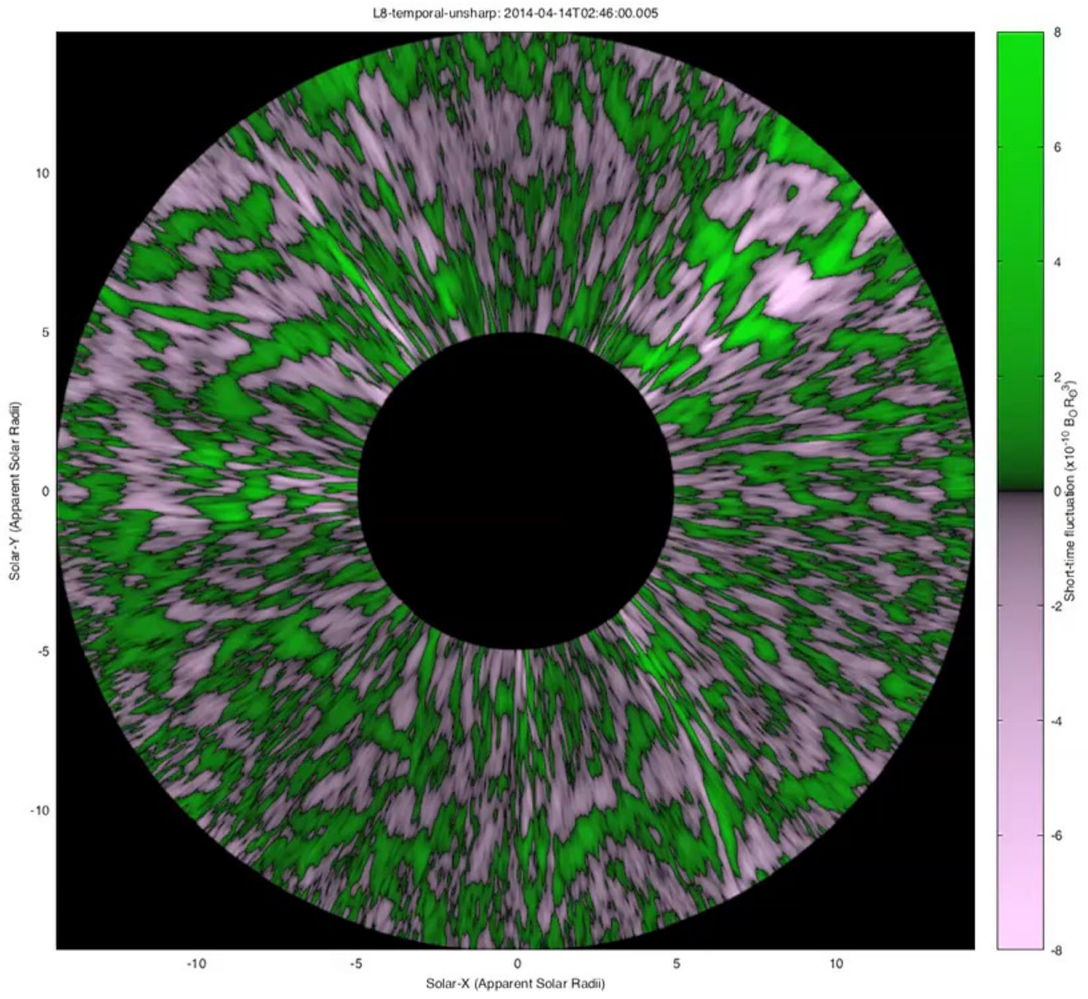

DeForest+ 2018

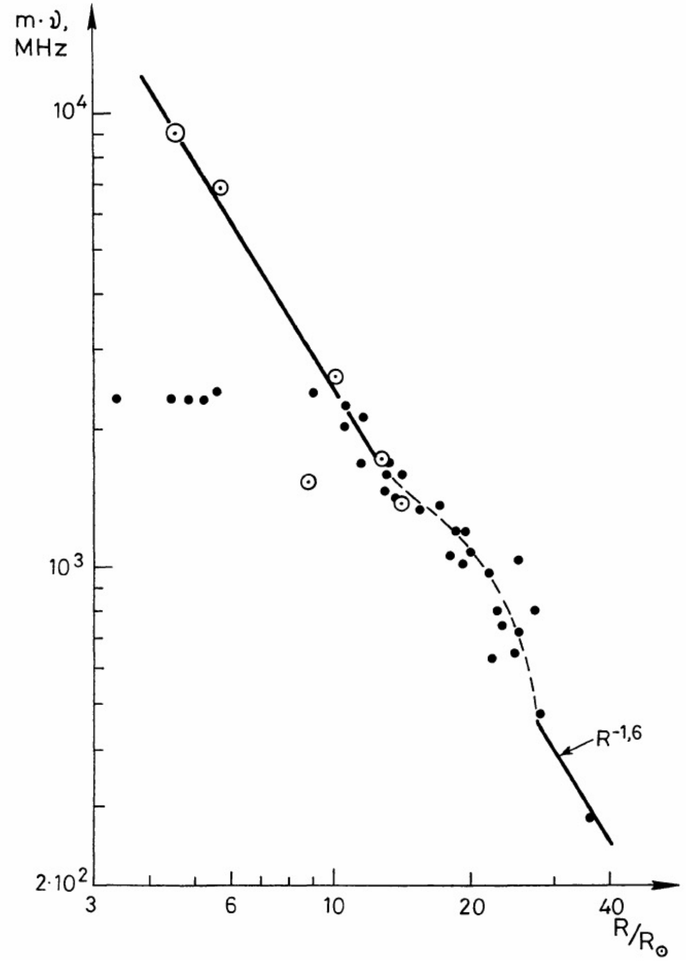

- Lotova+ (1985, 1997) region of enhanced scintillation $\sim 10 - 30\ R_\odot$
- Density fluctuations imply fluctuations in V_A

Corrugated Alfven surface - In situ observations

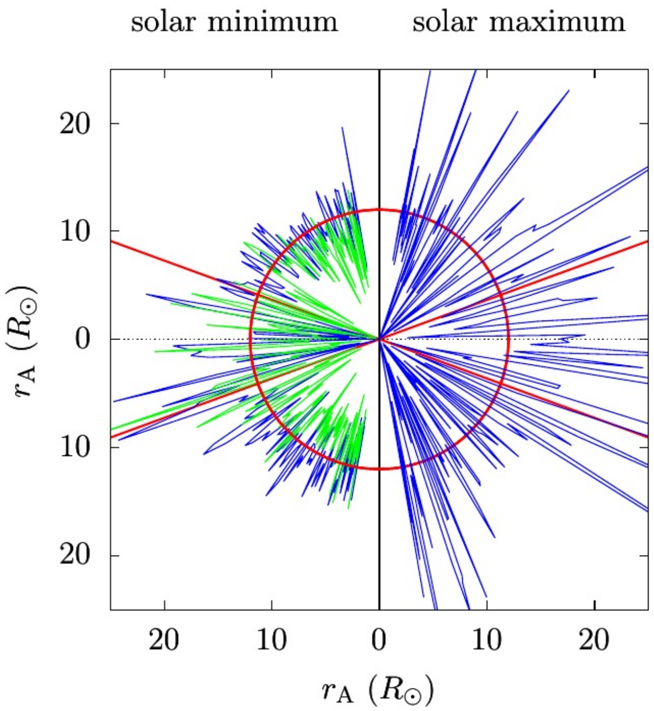

Verscharen+ 2021; *Ulysses* data

PSP E2

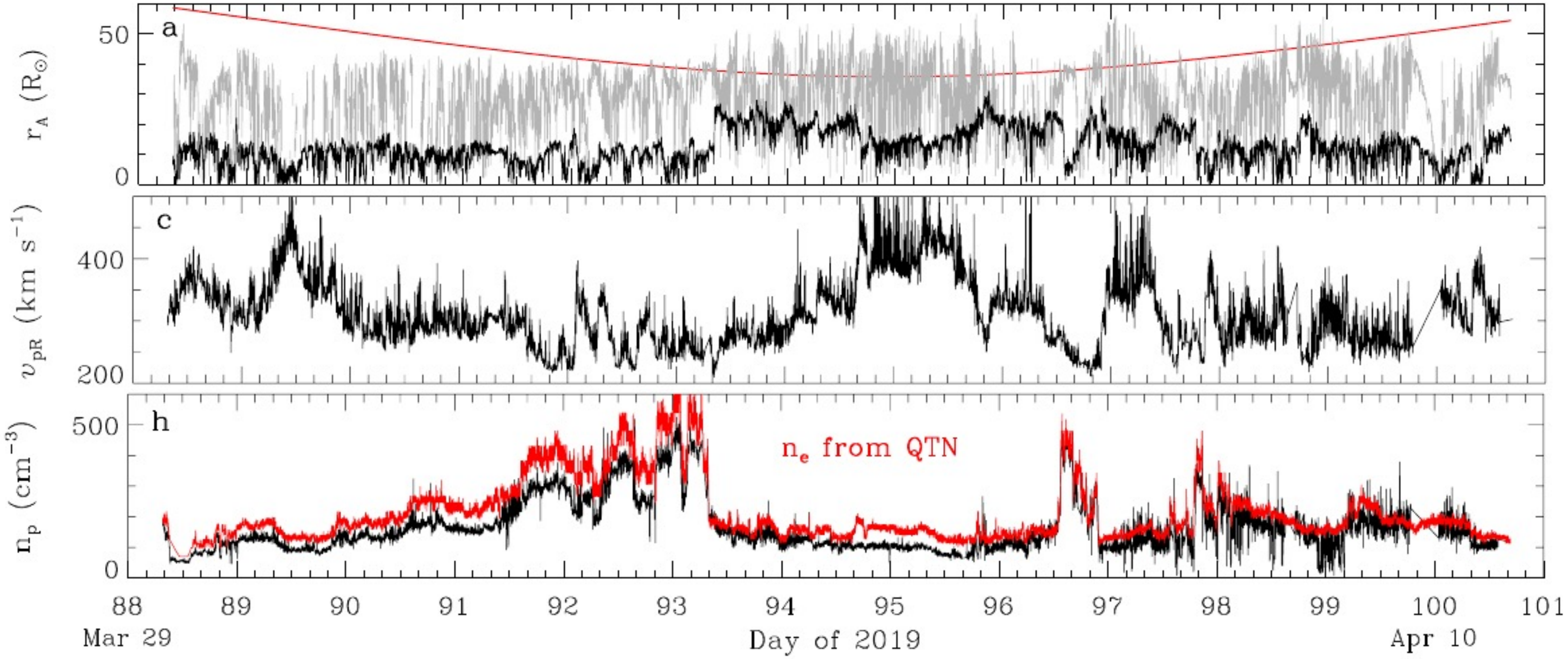

Liu+ 2021; *PSP* data

Corrugated Alfven surface - combined in-situ & remote observations

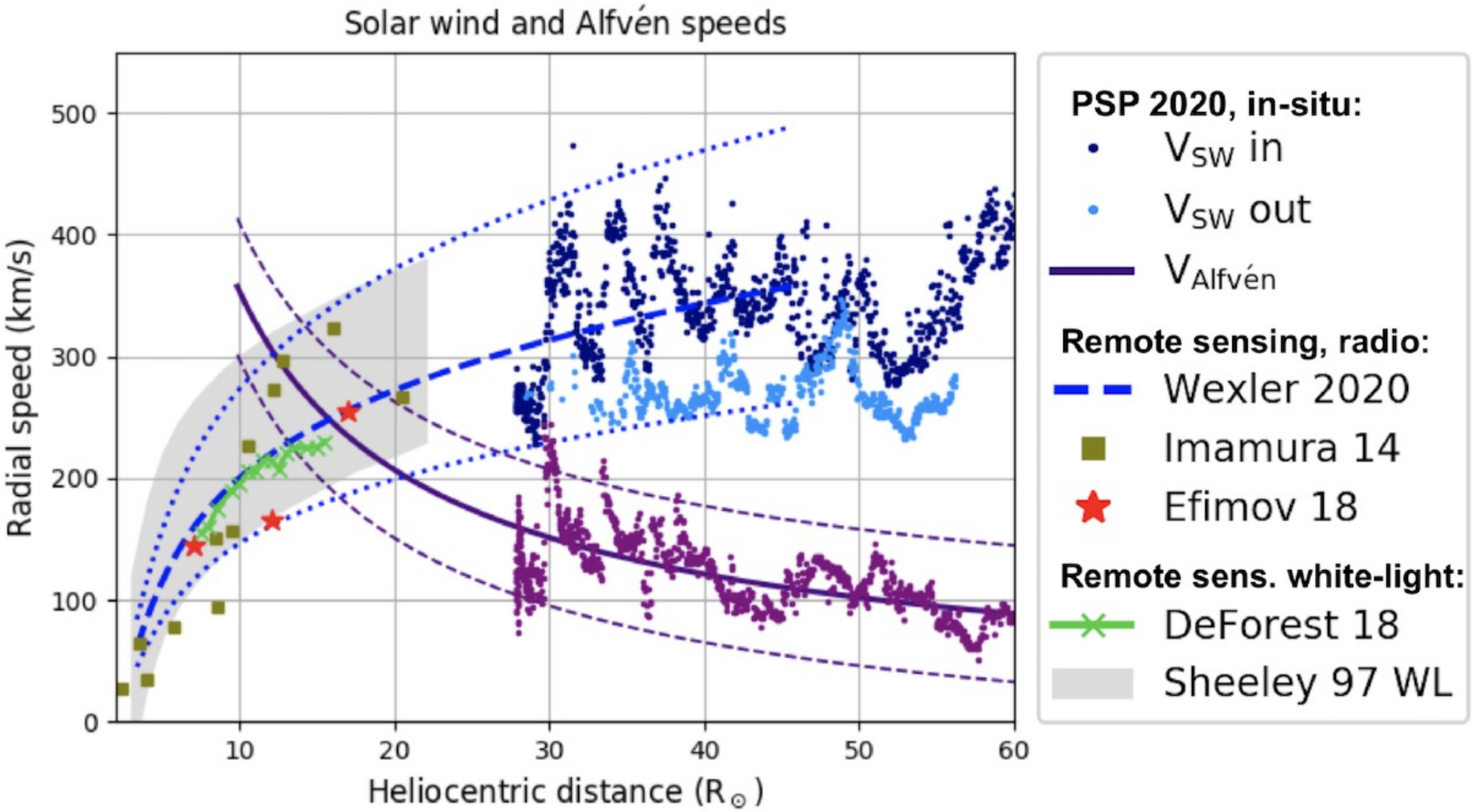

- Wexler+ (2020) used 600 s averages of PSP measurements
- $r_A \sim 10 - 27\ R_\odot$

Global simulation with turbulence modeling – Schematic of Reynolds-Averaging Approach

Reynolds decomposition splits fields (ã) into mean (a) and fluctuation (a'; arbitrary amplitude): $\tilde{\mathbf{a}} = \mathbf{a} + \mathbf{a}'$

Explicitly resolve large-scale/mean flow

Large scale (mean field) model equations:
- Momentum
- Magnetic field
- Density
- internal energies (Te & Tp)
- additional species (PUIs, interstellar H)

NEW TERMS:
- Fluctuation pressure
- Reynolds stresses
- Turbulent electric field
- Heat function/dissipation

Closures:
- **Eddy viscosity (kinetic & magnetic)**
- **Production/mixing terms**
- **Turbulent transport coefficients**

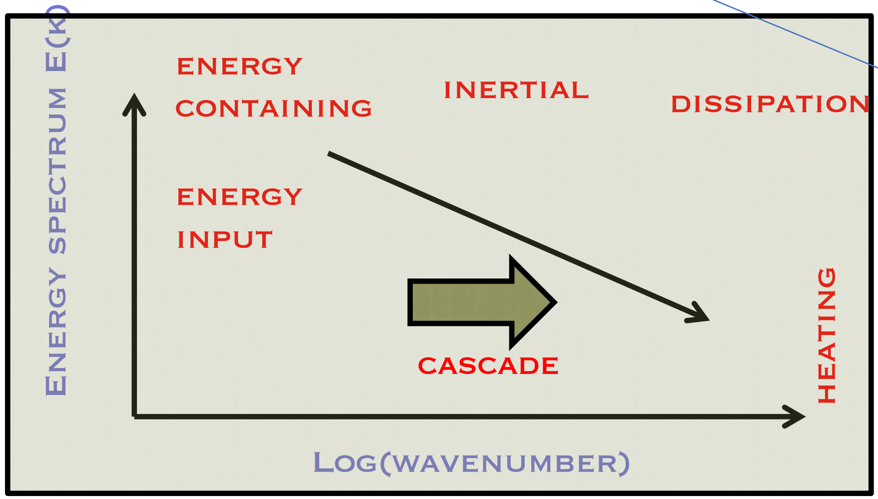

Evaluate required turbulence parameters:
Transport equations for energy, cross helicity, correlation scales

Describe fluctuations statistically

Plasma kinetic theory:
- branching between e/p heating

Usmanov+ 2018, ApJ

Global sim w' turbulence modeling – Comparison with five PSP orbits

$$Z^2 = \langle v'^2 + b'^2 \rangle$$

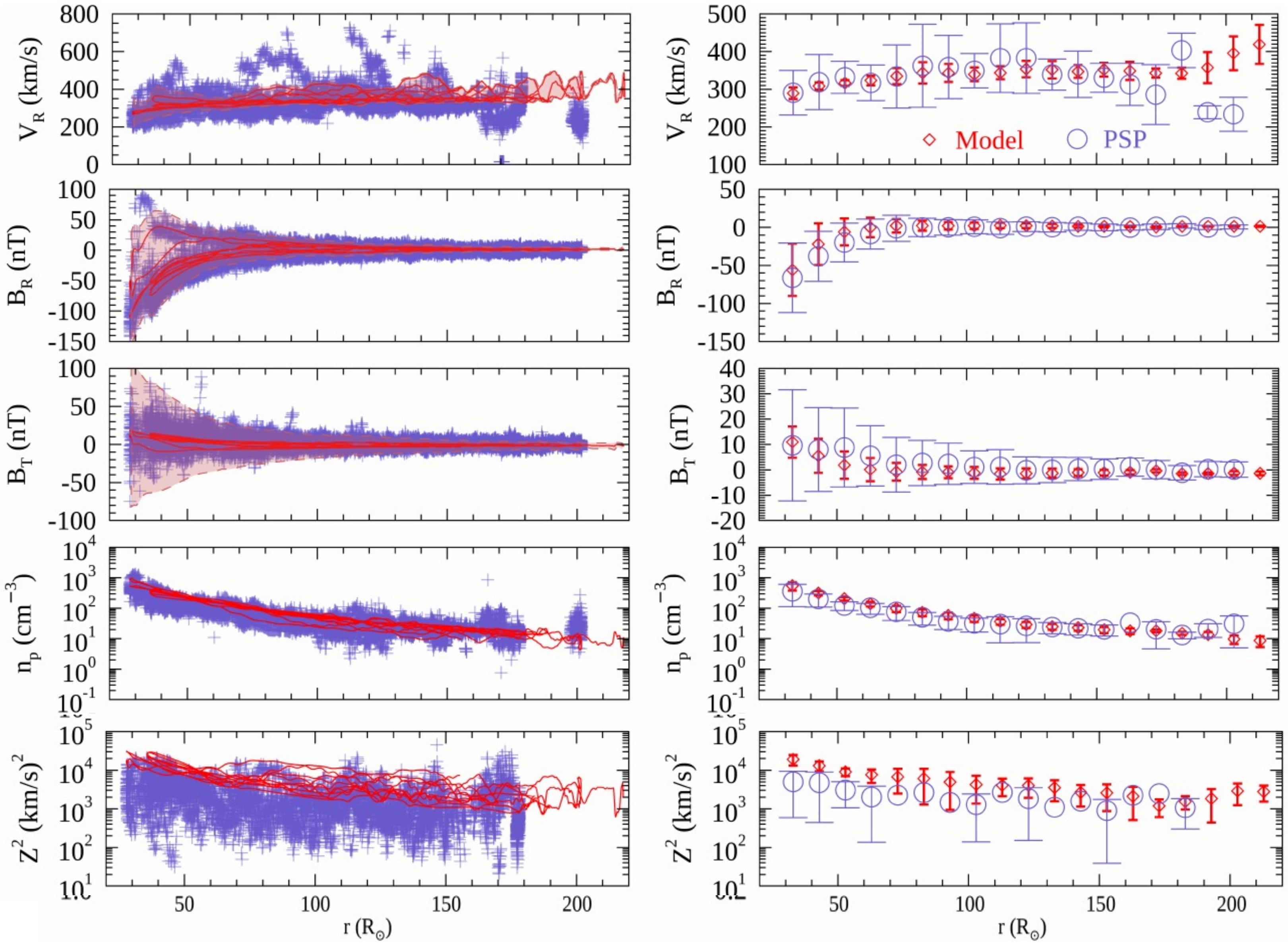

Chhiber+ 2021, in press @ ApJ

Alfven surface from 10 deg dipole run

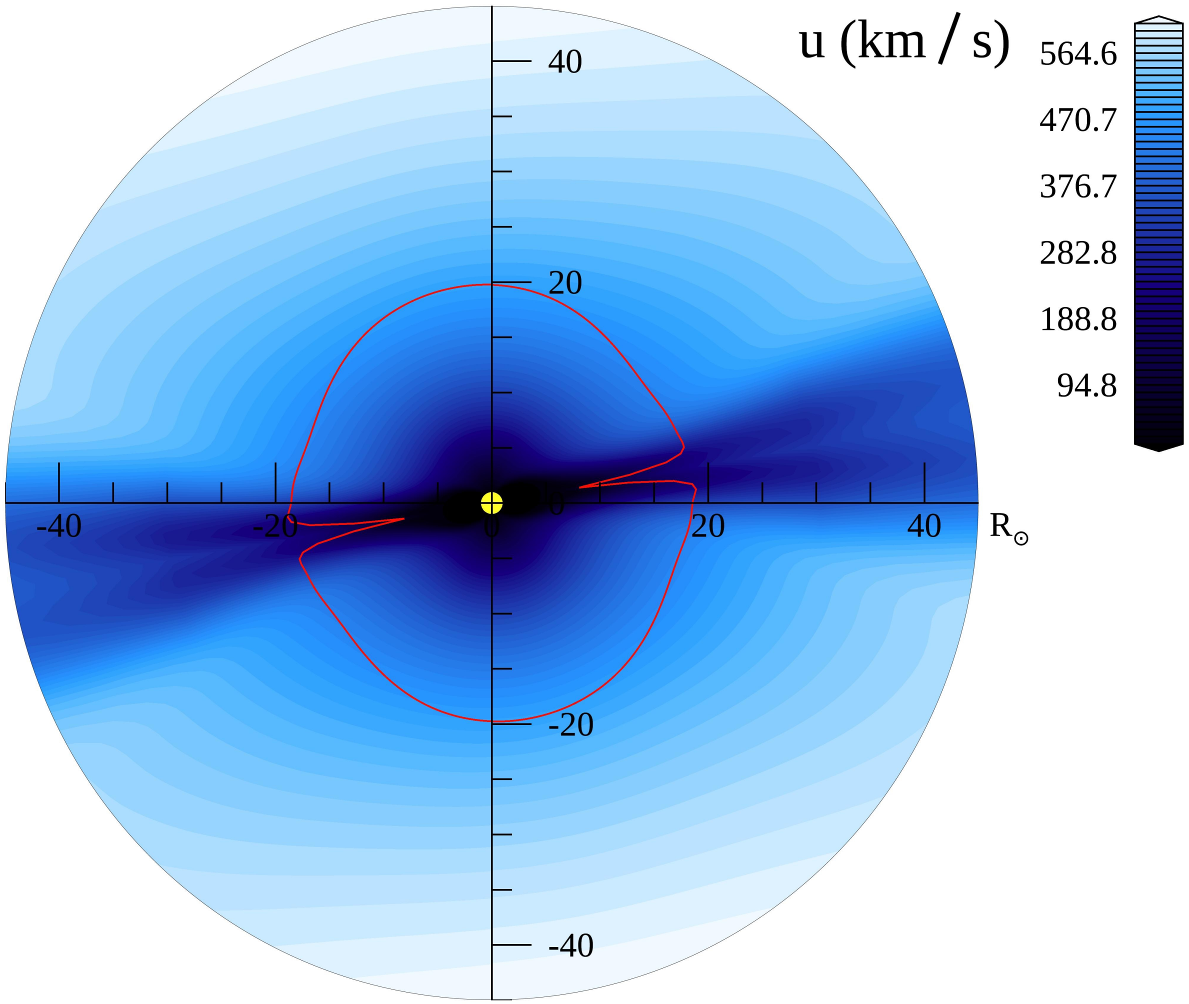

- $V_A = B/\sqrt{4\pi\rho}$
- Assume a reasonable Alfven ratio ($r_A = \delta u^2/\delta B^2$); convert Z^2 to rms velocity and magnetic fluctuations

Alfven zone (with magnetic turbulence envelope)

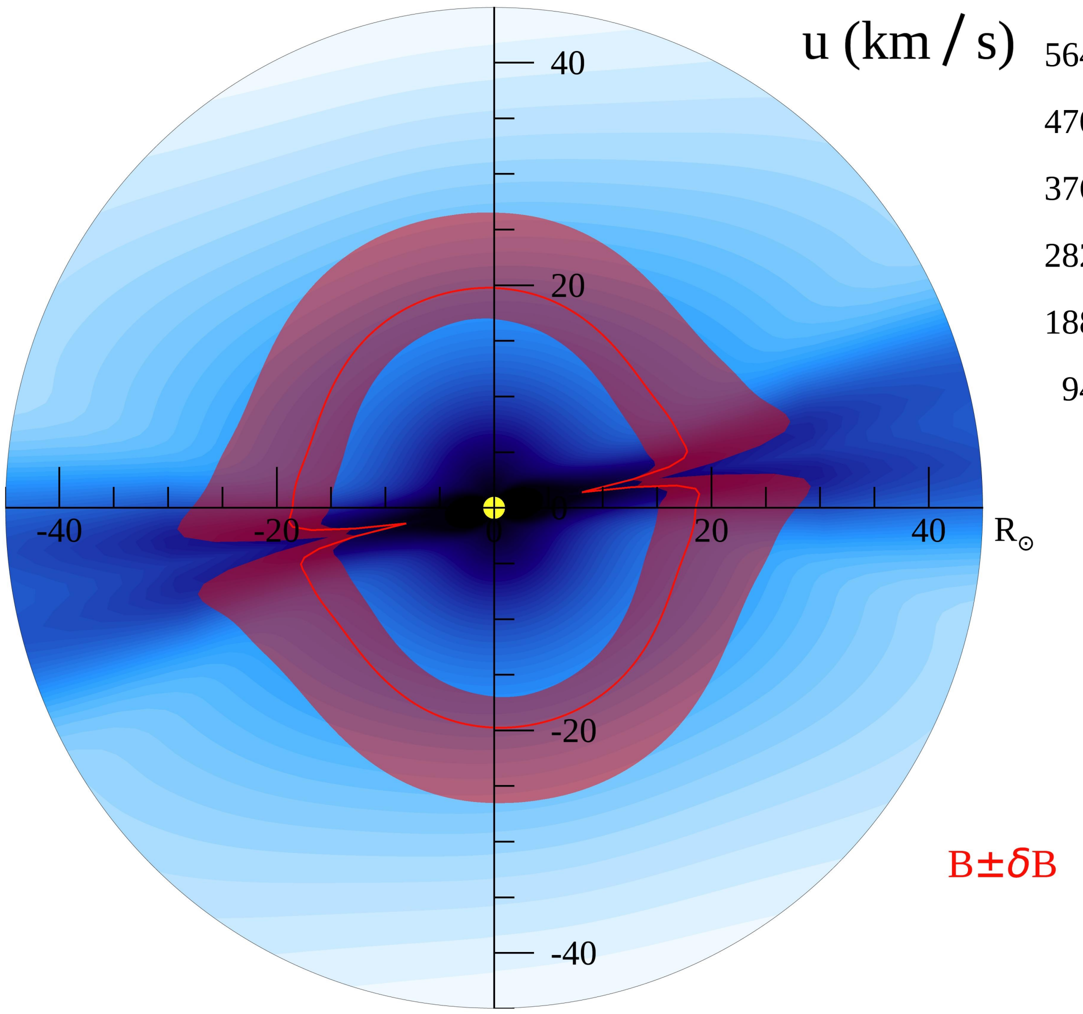

- $V_A = B/\sqrt{4\pi\rho}$
- Assume a reasonable Alfven ratio ($r_A = \delta u^2/\delta B^2$); convert Z^2 to rms velocity and magnetic fluctuations

Alfven zone (with magnetic/flow turbulence envelopes)

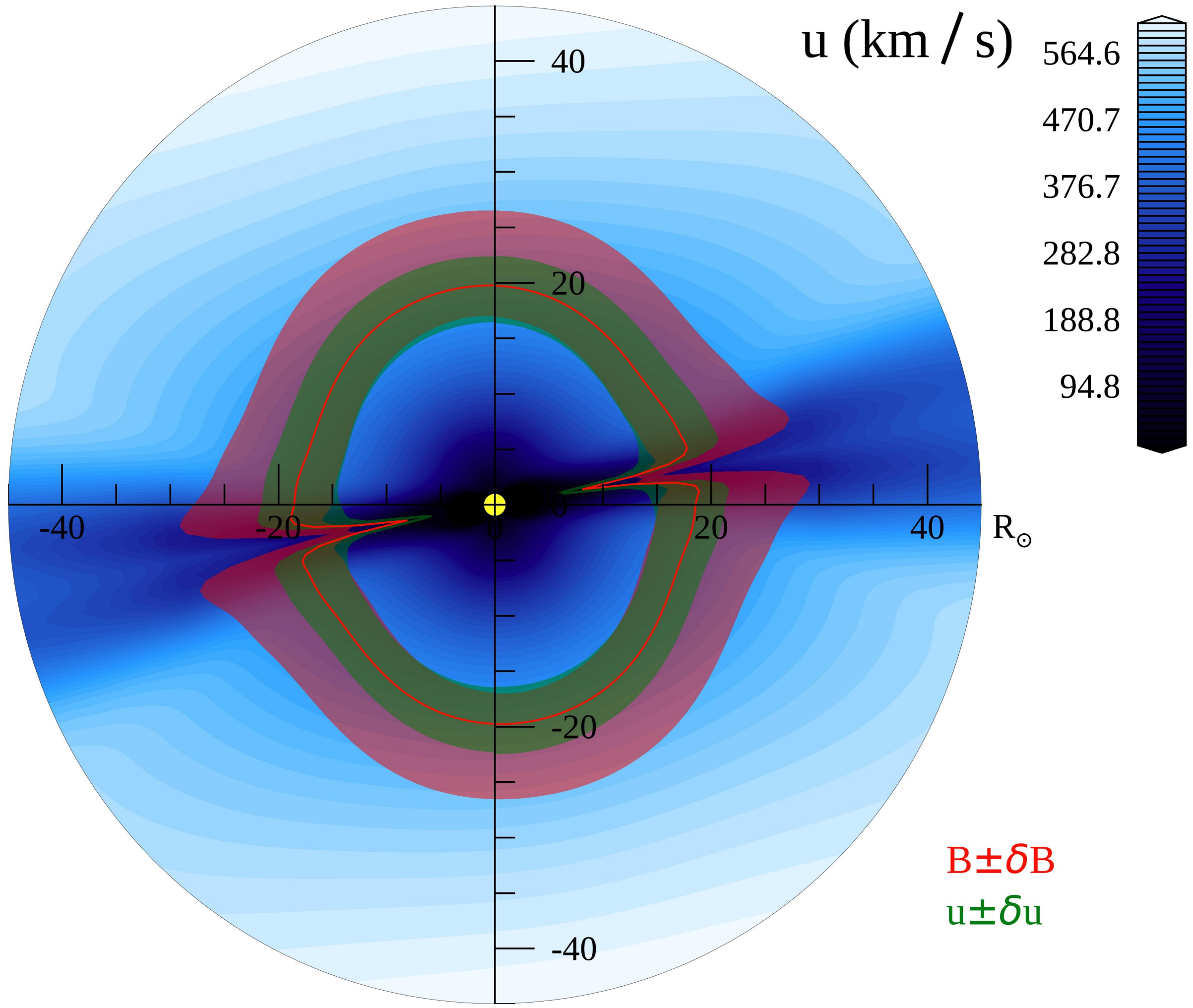

- $V_A = B/\sqrt{4\pi\rho}$
- Assume a reasonable Alfven ratio ($r_A = \delta u^2/\delta B^2$); convert Z^2 to rms velocity and magnetic fluctuations

Alfven zone (with magnetic and flow turbulence envelopes)

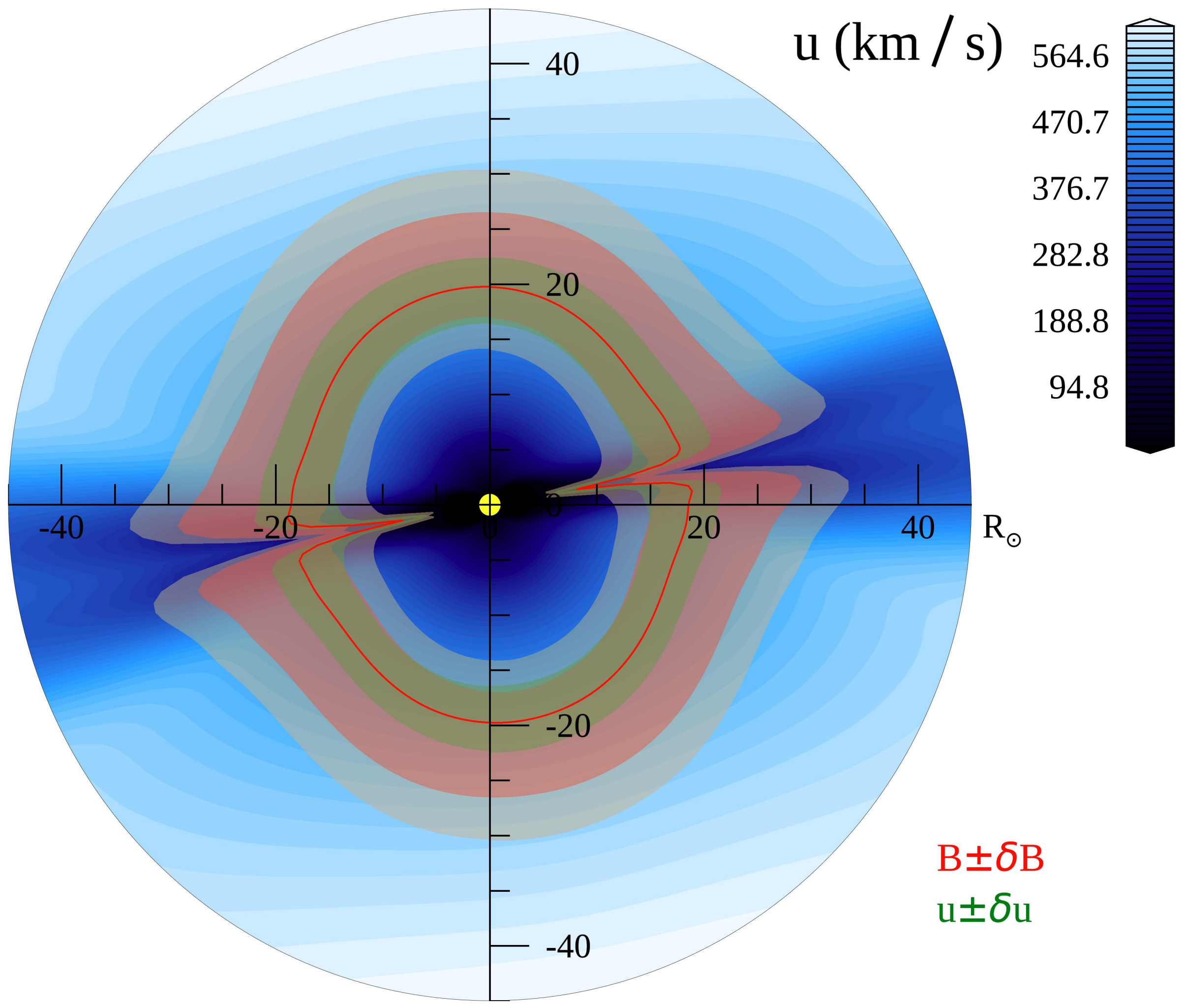

- $V_A = B/\sqrt{4\pi\rho}$
- Assume a reasonable Alfven ratio ($r_A = \delta u^2/\delta B^2$); convert Z^2 to rms velocity and magnetic fluctuations

- Lotova enhanced radio scintillation/fluctuations at $15 - 30\ R_\odot$
- Variability from local fluctuations, not large-scale source-related variations

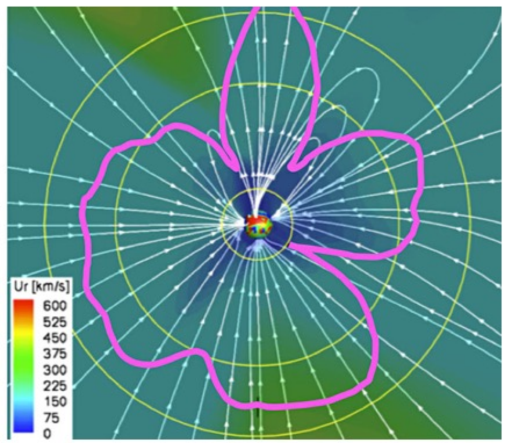

Alfven zone (with turbulence envelopes)

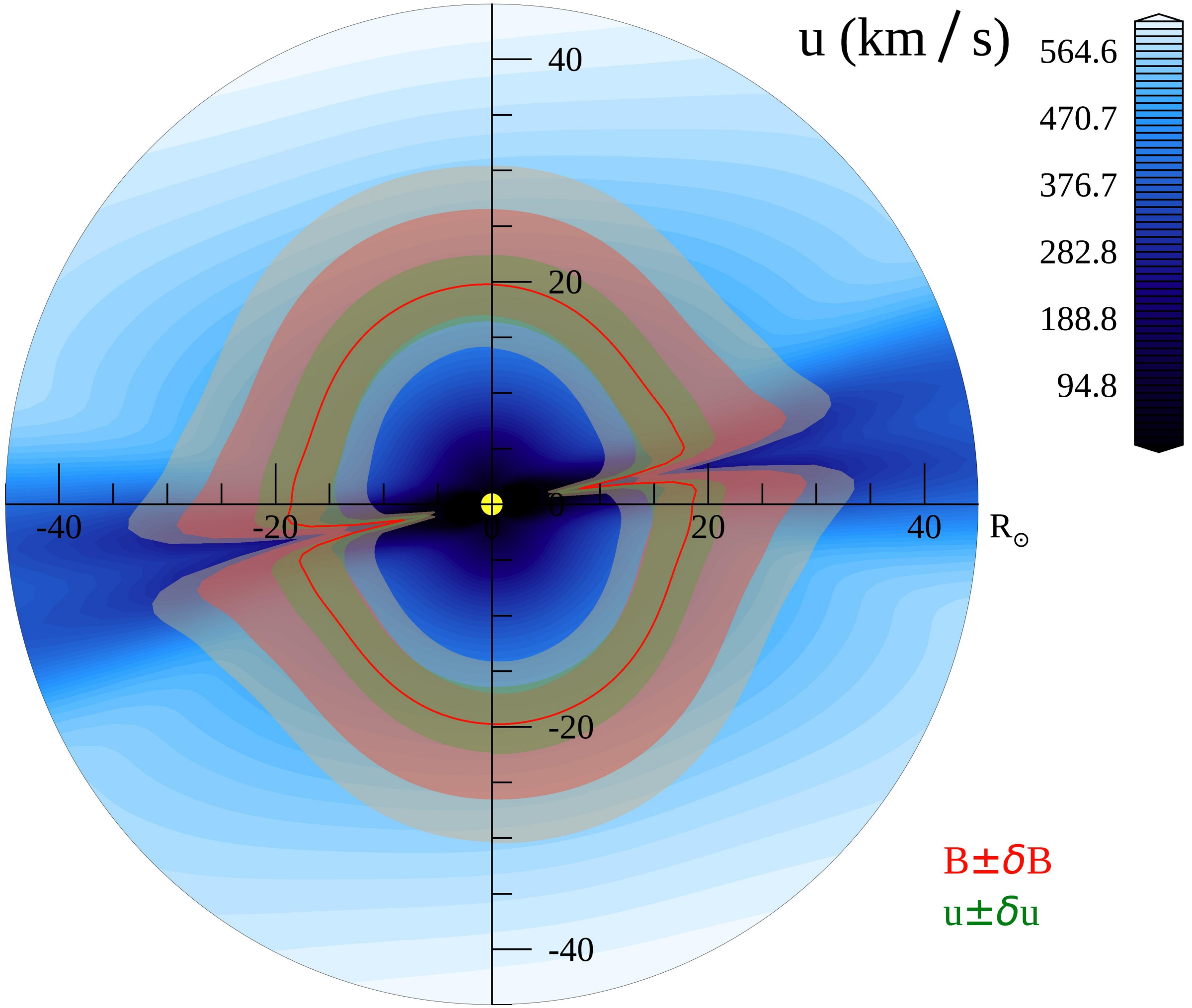

- $V_A = B/\sqrt{4\pi\rho}$
- Assume a reasonable Alfven ratio ($r_A = \delta u^2/\delta B^2$); convert Z^2 to rms velocity and magnetic fluctuations

- Lotova enhanced radio scintillation/fluctuations at $15 - 30\ R_\odot$
- Variability from local fluctuations, not large-scale source-related variations

Explicit fluctuations -

- at each grid point a random magnetic fluctuation is drawn from a Gaussian distribution constrained by model
- Dist. has standard dev. equal to local δB at that grid point

Corrugated Alfven zone (with explicit fluctuations)

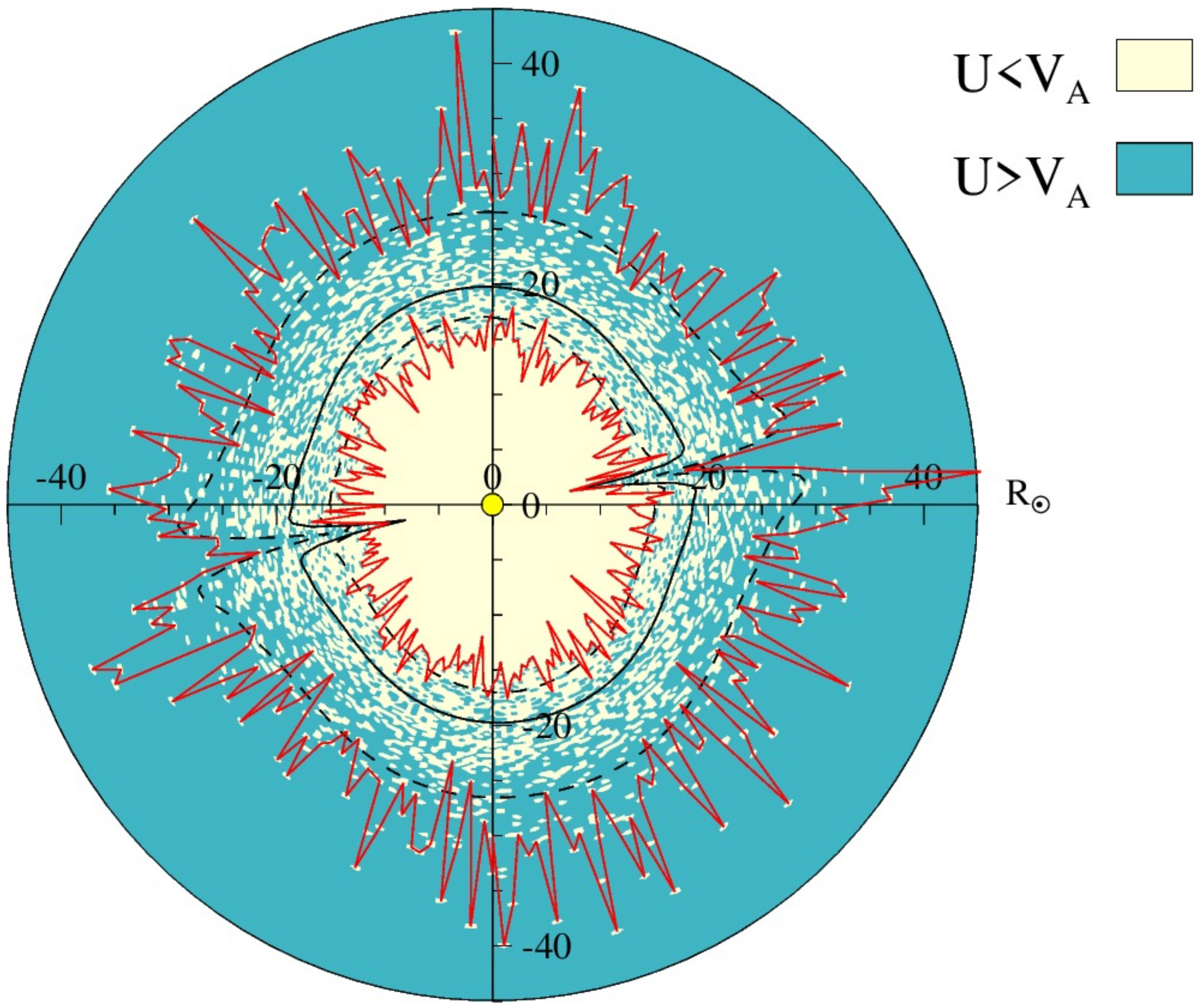

Explicit fluctuations -

- at each grid point a random magnetic fluctuation is drawn from a Gaussian distribution constrained by model
- Dist. has standard dev. equal to local δB at that grid point
- Can use velocity or density fluctuations too, in principle

Musings on “fractal” Alfven zone

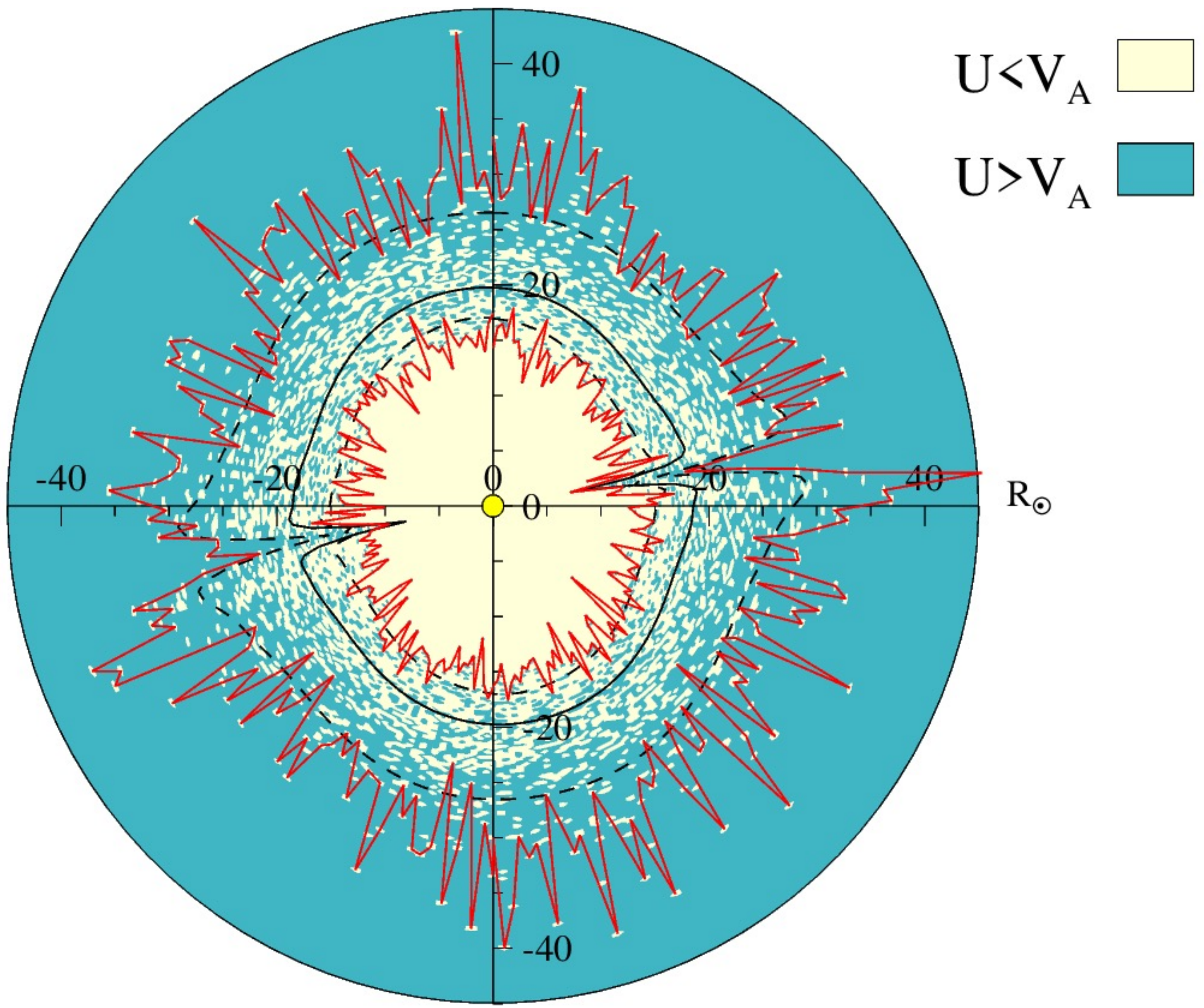

Fractal nature –

- How long is the coast of Britain? - Mandelbrot

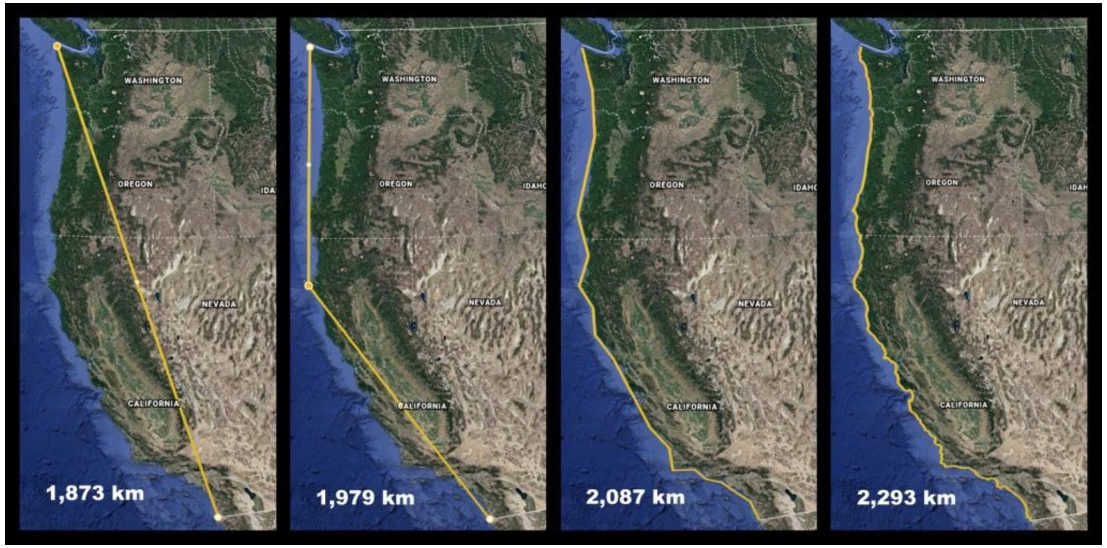

Musings on "fractal" Alfven zone

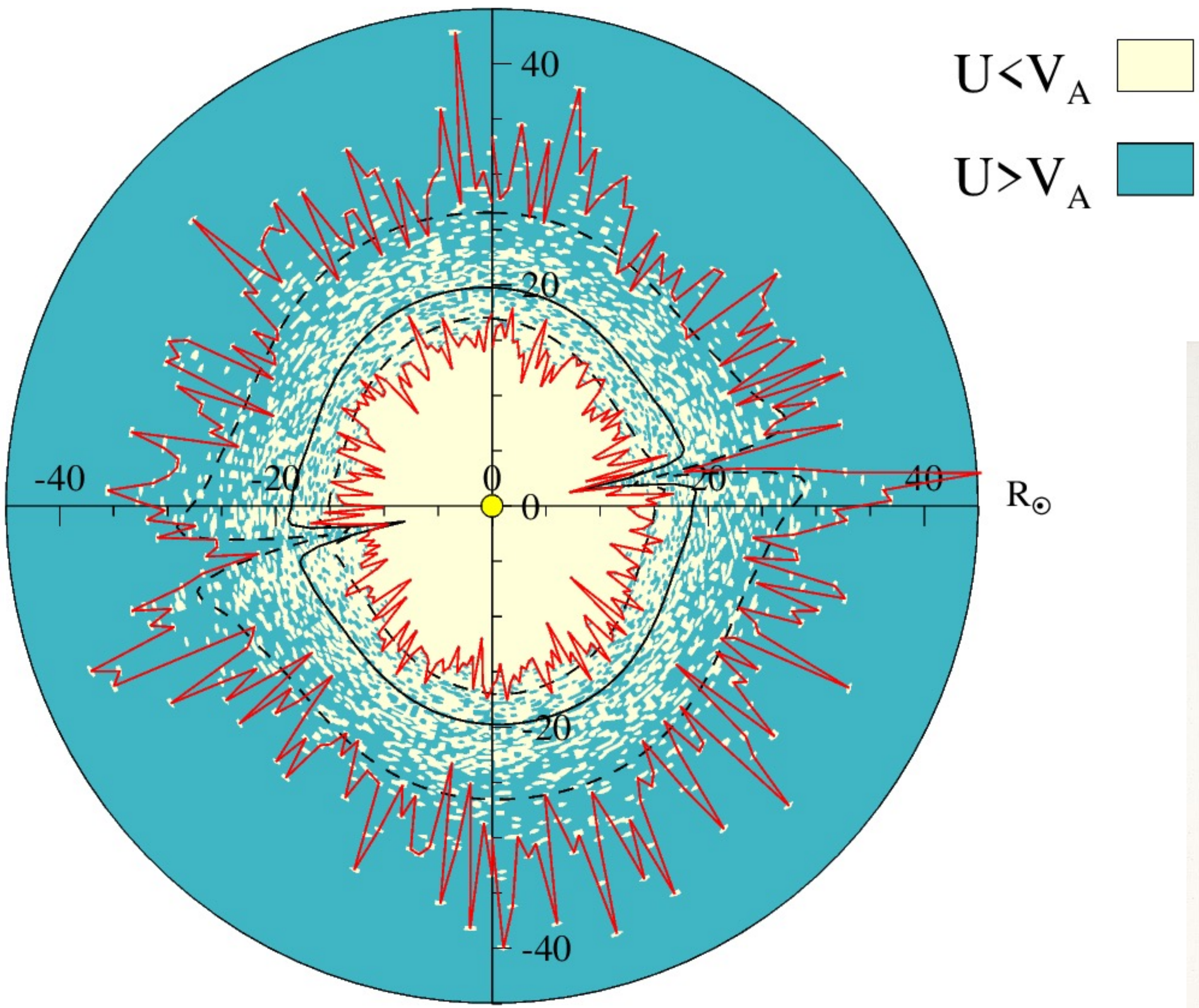

Fractal nature –

- How long is the coast of Britain? - Mandelbrot
- More like 1000 Islands, NY
- First/inner Alfven surface, and final/outer Alfven surface

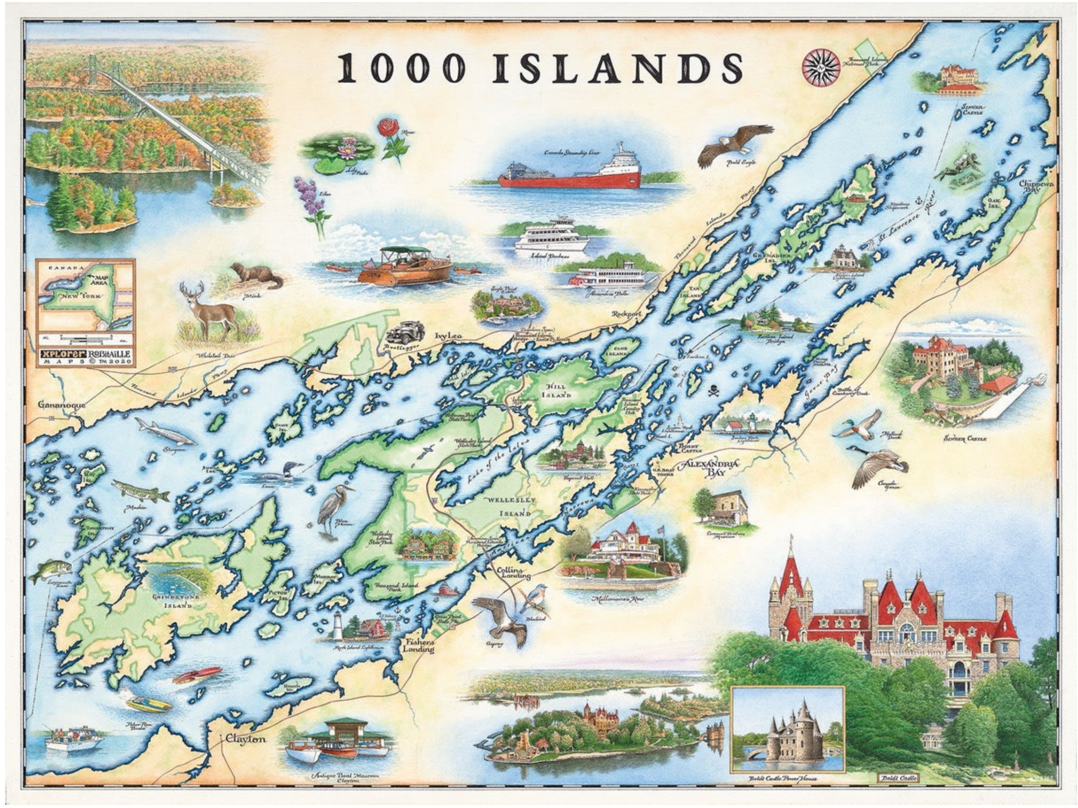

Corrugated/“fractal” Alfven zone (with explicit fluctuations)

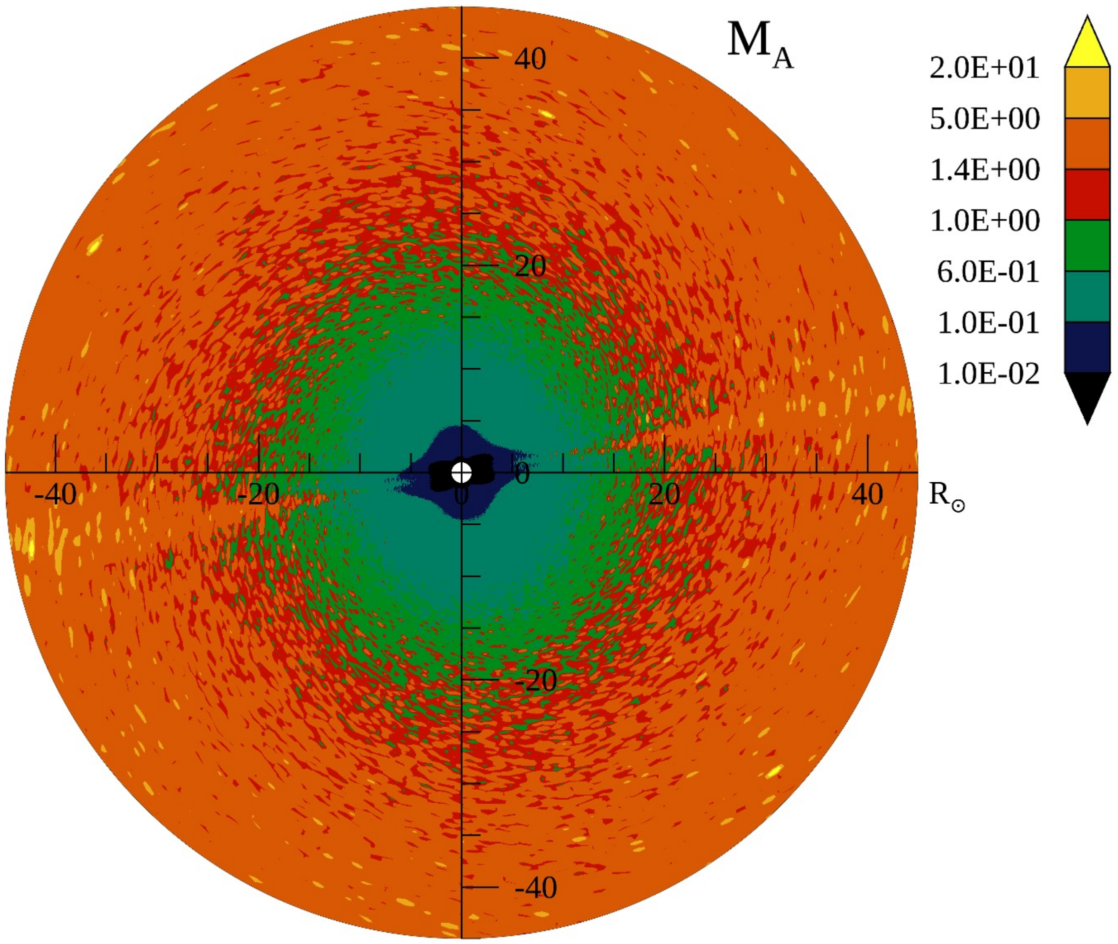

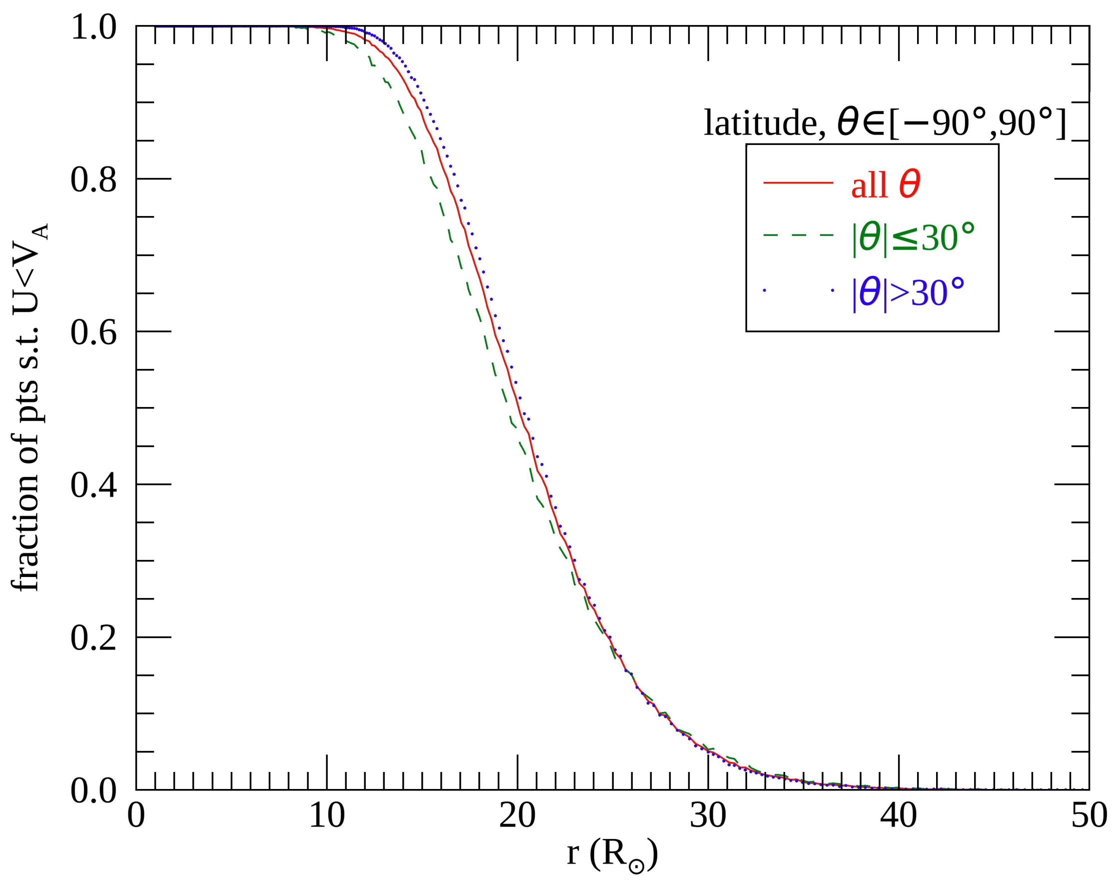

Fraction of points that are sub-Alfvenic at different *r*

Corrugated/“fractal” Alfven zone – solar min (left) and max (right)

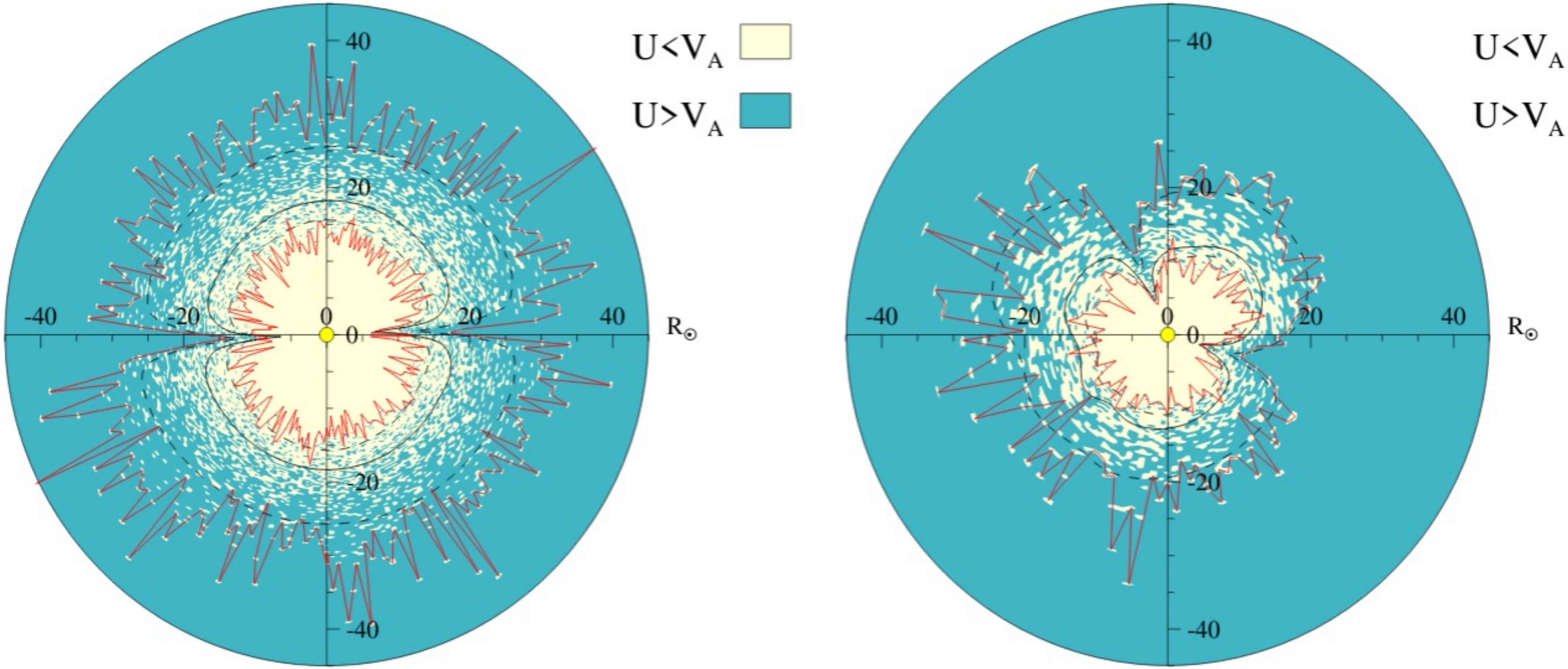

Corrugated Alfven zone – comparison with PSP

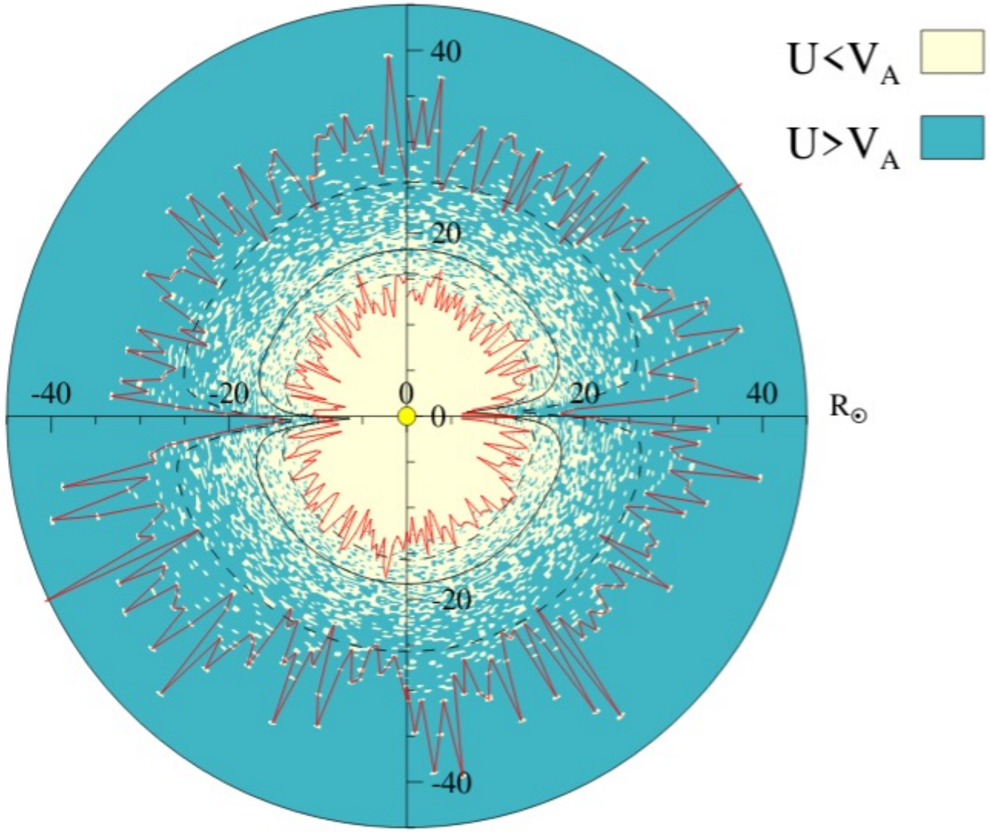

- Virtual PSP trajectory along sim driven by Nov 2018 magnetogram
- PSP data at 1-hr cadence

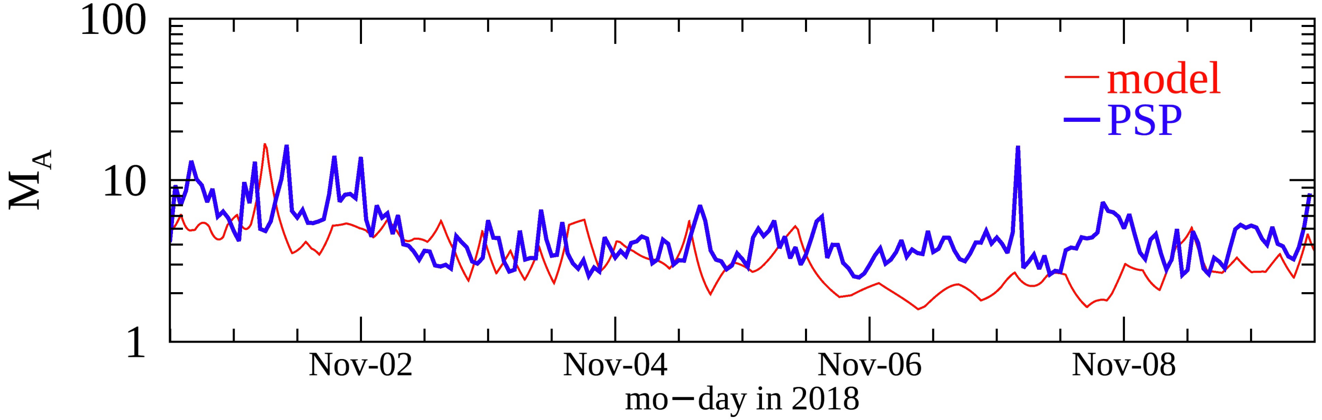

Discussion

- Turbulence implies an extended spatial region of transition from sub to super Alfvenic flow
- Enhanced heating/dissipation; nonlinear interactions of inward and outward propagating modes; enhanced SEP scattering.. See Bill Matthaeus' slides later today
- Can PUNCH detect inward/outward modes over this extended zone?
- Angular momentum loss of Sun – In Weber & Davis (1967) picture r_A is “lever arm” of the corona… impact of turbulent variability? Usmanov+ 2018 showed that statistical turbulence reduces ang. mom. loss rate
- Effects of solar activity on Alfven surface – discrepancy between models and observations

Summary

- In addition to large-scale variability and solar-cycle effects, smaller scale structure are suggested by recent observations
- 3D global simulations with turbulence modeling are a useful tool to examine these effects
- Alfven zone - statistical envelopes bounded by rms fluctuations
- Corrugated first/final Alfven surface... "fractal" Alfven zone with blobs of sub/super-Alfvenic wind
- Future observations by PSP (may have already sampled Alfven zone…) and PUNCH will shed more light on the accuracy of this picture

Extra Slides

Spatial Scales Resolved in Simulations

- Resolution ~ $700\times120\times240$ in r, θ, ϕ ($r = 1\ R_\odot$ - 5 AU)
- Grid scale Δ is generally within a factor of few correlation scales

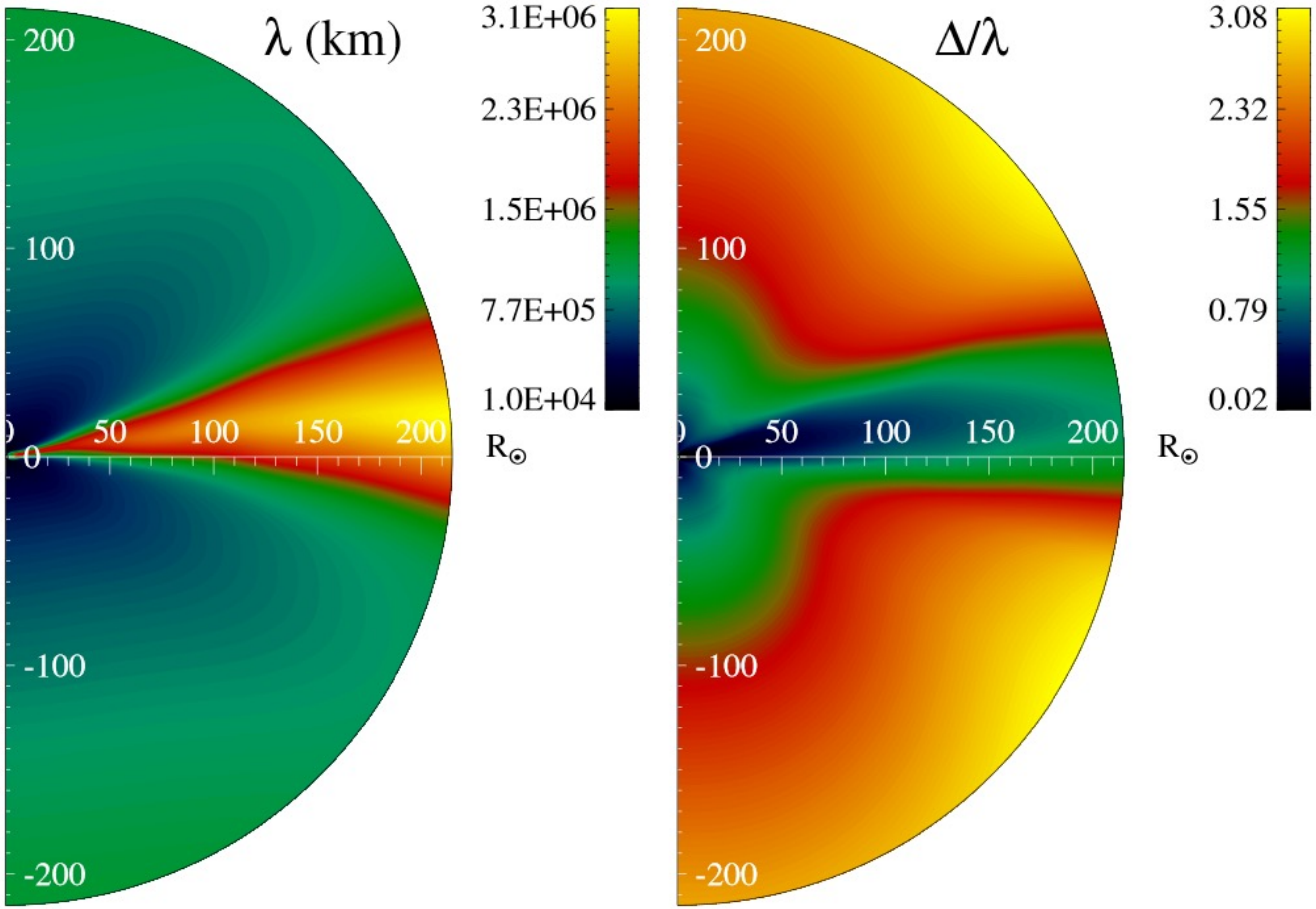

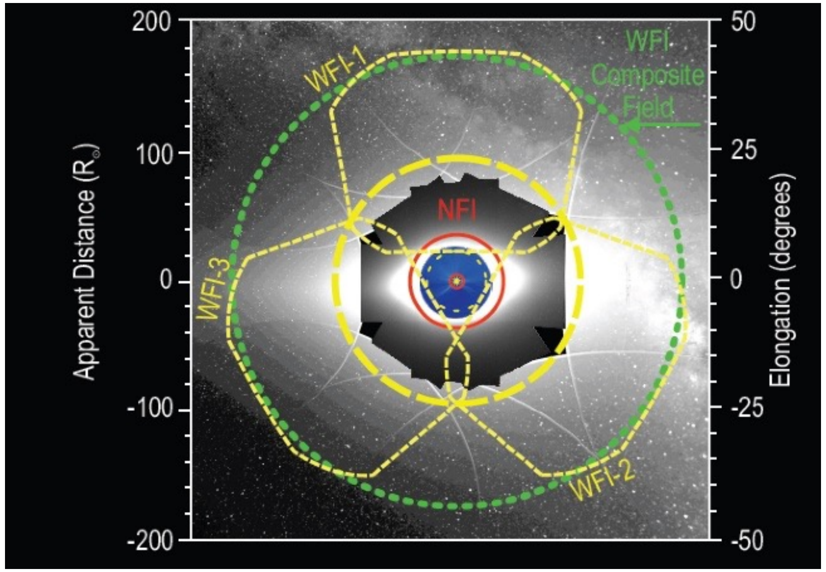

PUNCH

- Very good coverage of large scales
- Coverage of onset of turbulence down to $\approx 0.25\ \lambda$ for observations at 50 R_s apparent distance

3D MHD simulations of global solar wind

Large-scale variability – solar-source related; solar activity effects

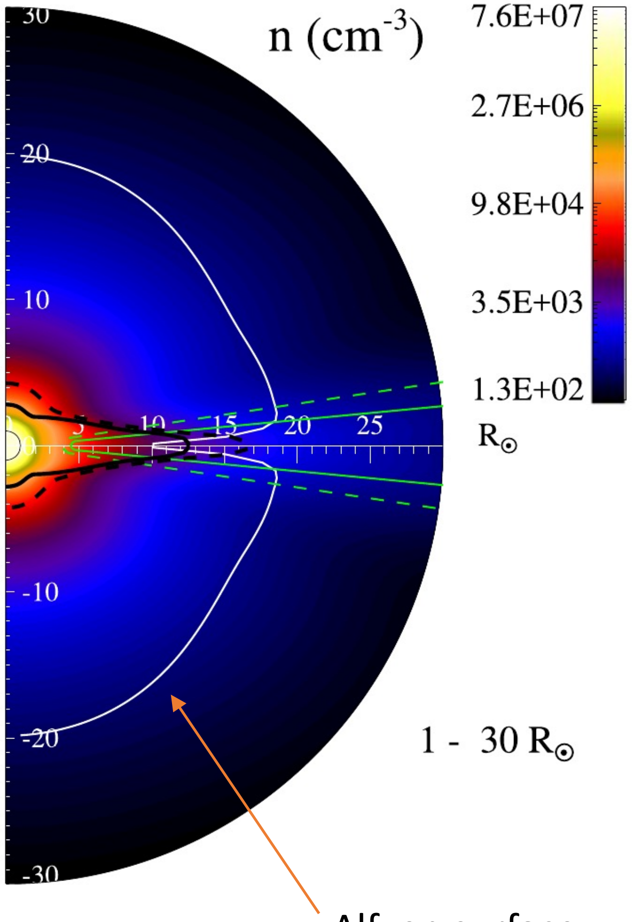

Untilted dipole; Chhiber+ 2019

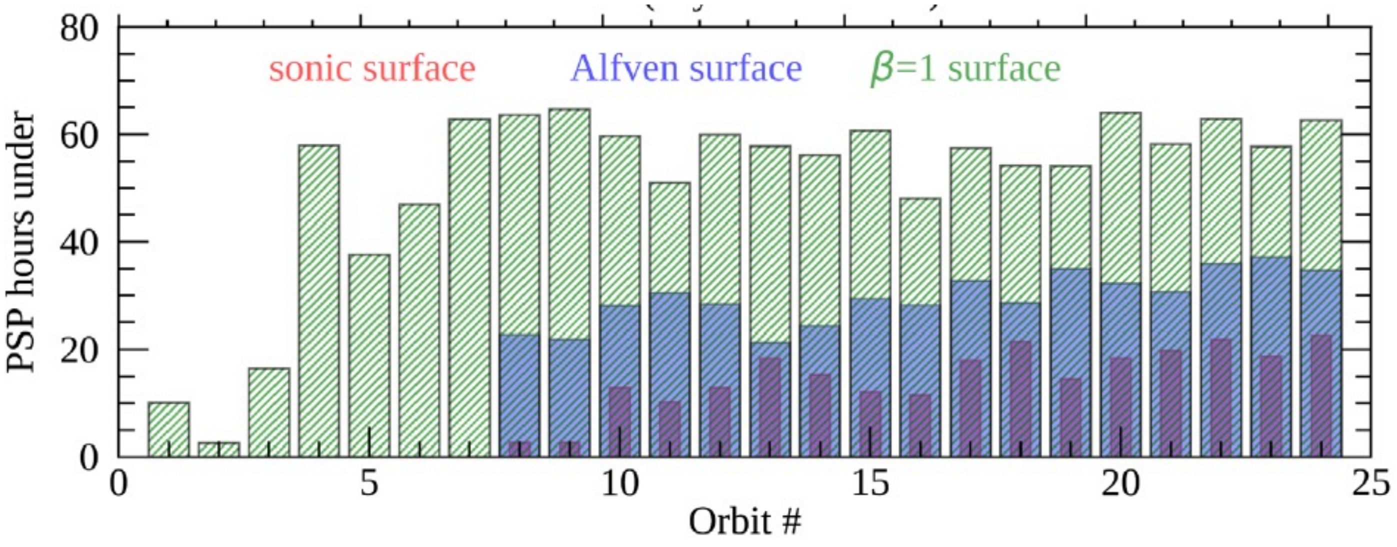

Context predictions for time PSP spends under critical surfaces

5-deg tilted dipole; Chhiber+ 2019

Two-Fluid Reynolds Averaged MHD Equations

$$\frac{\partial \rho}{\partial t} + \nabla \cdot (\rho \mathbf{v}) = 0$$

$$\frac{\partial(\rho \mathbf{u})}{\partial t} + \nabla \cdot \left[\rho \mathbf{v} \mathbf{u} - \frac{1}{4\pi} \mathbf{B}\mathbf{B} + \left(P_S + P_E + \frac{B^2}{8\pi} + \frac{\langle B'^2 \rangle}{8\pi} \right) \mathbf{I} + \boldsymbol{\mathcal{R}} \right] = -\rho \left(\frac{G M_\odot}{r^2} + \boldsymbol{\Omega} \times \mathbf{u} \right)$$

$$\frac{\partial \mathbf{B}}{\partial t} = \nabla \times \left(\mathbf{v} \times \mathbf{B} + \boldsymbol{\varepsilon}_m \sqrt{4\pi\rho} \right)$$

$$\frac{\partial P_S}{\partial t} + (\mathbf{v} \cdot \nabla) P_S + \gamma P_S \nabla \cdot \mathbf{u} + (\gamma - 1) \frac{P_S - P_E}{\tau_{SE}} = f_p Q_T$$

$$\frac{\partial P_E}{\partial t} + (\mathbf{v} \cdot \nabla) P_E + \gamma P_E \nabla \cdot \mathbf{u} + (\gamma - 1) \left[\frac{P_E - P_S}{\tau_{SE}} + \nabla \cdot \mathbf{q}_H \right] = (1 - f_p) Q_T$$

- P_S and P_E are the proton and electron pressure
- $\mathbf{u}$ is the velocity in the inertial frame
- $\mathbf{v}$ is the velocity in the rotating frame
- τ_{SE} is the electron-proton Coulomb collision rate
- $\boldsymbol{\mathcal{R}} = \langle \rho \mathbf{v}'\mathbf{v}' - \frac{\mathbf{B}'\mathbf{B}'}{4\pi} \rangle$ is the Reynolds stress tensor
- $\boldsymbol{\varepsilon}_m = \frac{\langle \mathbf{v}' \times \mathbf{B}' \rangle}{(4\pi\rho)^{1/2}}$ is the mean turbulent electric field
- Q_T is the turbulent heating rate
- $\mathbf{q}_H$ is the electron heat flux

Two-Fluid Reynolds-averaged MHD with Turbulence Transport

- Turbulence transport equations obtained by subtracting mean-flow eqns. from full eqns., and averaging.

mean flow

$$\frac{\partial \rho}{\partial t} + \nabla \cdot (\rho \mathbf{v}) = 0$$

$$\frac{\partial (\rho \mathbf{u})}{\partial t} + \nabla \cdot \left[\rho \mathbf{v}\mathbf{u} - \frac{1}{4\pi}\mathbf{B}\mathbf{B} + \left(P_S + P_E + \frac{B^2}{8\pi} + \frac{\langle B'^2 \rangle}{8\pi} \right)\mathbf{I} + \boldsymbol{\mathcal{R}} \right] = -\rho \left(\frac{GM_\odot}{r^2} + \boldsymbol{\Omega} \times \mathbf{u} \right)$$

$$\frac{\partial \mathbf{B}}{\partial t} = \nabla \times (\mathbf{v} \times \mathbf{B} + \boldsymbol{\varepsilon}_m \sqrt{4\pi\rho})$$

$$\frac{\partial P_S}{\partial t} + (\mathbf{v} \cdot \nabla) P_S + \gamma P_S \nabla \cdot \mathbf{u} + (\gamma - 1)\frac{P_S - P_E}{\tau_{SE}} = f_p Q_T$$

$$\frac{\partial P_E}{\partial t} + (\mathbf{v} \cdot \nabla) P_E + \gamma P_E \nabla \cdot \mathbf{u} + (\gamma - 1)\left[\frac{P_E - P_S}{\tau_{SE}} + \nabla \cdot \mathbf{q}_H \right] = (1 - f_p) Q_T$$

turbulence

$$\frac{\partial Z^2}{\partial t} + (\mathbf{v} \cdot \nabla) Z^2 + \frac{(1 - \sigma_D) Z^2}{2} \nabla \cdot \mathbf{u} + \frac{2}{\rho} \boldsymbol{\mathcal{R}} : \nabla \mathbf{u} + 2\boldsymbol{\varepsilon}_m \cdot (\nabla \times \mathbf{u}) - (\mathbf{V}_A \cdot \nabla)(Z^2 \sigma_c) + Z^2 \sigma_c \nabla \cdot \mathbf{V}_A = -\frac{\alpha f^+(\sigma_c) Z^3}{\lambda}$$

$$\frac{\partial (Z^2 \sigma_c)}{\partial t} + (\mathbf{v} \cdot \nabla)(Z^2 \sigma_c) + \frac{Z^2 \sigma_c}{2} \nabla \cdot \mathbf{u} + \frac{2}{\rho} \boldsymbol{\mathcal{R}} : \nabla \mathbf{V}_A + 2\boldsymbol{\varepsilon}_m \cdot (\nabla \times \mathbf{u}) - (\mathbf{V}_A \cdot \nabla) Z^2 + (1 - \sigma_D) Z^2 \nabla \cdot \mathbf{V}_A = -\frac{\alpha f^-(\sigma_c) Z^3}{\lambda}$$

$$\frac{\partial \lambda}{\partial t} + (\mathbf{v} \cdot \nabla)\lambda = \beta f^+(\sigma_c) Z$$

- $Z^2 = \langle v'^2 + b'^2 \rangle$ is (twice the incompressible yurbulent energy per unit mass
- $\sigma_c = \dfrac{2\langle \mathbf{v}' \cdot \mathbf{b}' \rangle}{\langle v'^2 + b'^2 \rangle}$ is the normalized cross helicity
- λ is the similarity (correlation) length scale

Turbulence modeling assumptions –
- Incompressible and transverse fluctuations
- Turbulent stresses modeled in terms of large-scale gradients (shear)
- NL terms modeled dimensionally (von Karman similarity)

- Physically and empirically motivated ICs and BCs
- Magnetogram-based or dipolar source magnetic field
- Numerical domain from coronal base to few AU

See Usmanov et al., 2018 for more details

Closures and other terms (extra slide)

- Electron-proton collision frequency:

$$\nu_E = \frac{8(2\pi m_e)^{1/2} e^4 N_E \ln\Lambda}{3 m_p (k_B T_E)^{3/2}} \qquad \ln\Lambda = \ln\left[\frac{3(k_B T_E)^{3/2}}{2\pi^{1/2} e^3 N_E^{1/2}}\right]$$

- Classical (Spitzer) electron heat conduction (below 5 $R_\odot$):

$$\mathbf{q}_\mathrm{S} = -\kappa \hat{\mathbf{B}}(\hat{\mathbf{B}}\cdot\nabla) T_E \qquad \kappa = 8.4\times 10^{-7}\, T_E^{5/2}$$

- Collisionless (Hollweg) heat conduction: $\mathbf{q}_\mathrm{H} = (3/2)\alpha_\mathrm{H} P_E \mathbf{v}$

- Turbulent heating: $Q_T = \dfrac{\alpha f^+(\sigma_c)\rho Z^3}{2\lambda}$

- TSDIA closure for turbulent stresses:

$$\boldsymbol{\varepsilon}_m = \bar{\alpha}\mathbf{B} - \bar{\beta}\nabla\times\mathbf{V}_A + \bar{\gamma}\nabla\times\mathbf{v}$$

$$\nu_M = (7/5)\bar{\gamma}$$

$$\nu_K = (7/5)\bar{\beta}$$

$$\frac{1}{\rho}\boldsymbol{\mathcal{R}} = \frac{2}{3}K_R\mathbf{I} - \nu_K\boldsymbol{\mathcal{S}} + \nu_M\boldsymbol{\mathcal{M}}$$

$$K_R = \sigma_D Z^2/2$$

$$\boldsymbol{\mathcal{S}} = \nabla\mathbf{u} + \nabla\mathbf{u}^T - \frac{2}{3}(\nabla\cdot\mathbf{u})\mathbf{I}$$

$$\boldsymbol{\mathcal{M}} = \nabla\mathbf{V}_A + \nabla\mathbf{V}_A^T - \frac{2}{3}(\nabla\cdot\mathbf{V}_A)\mathbf{I}$$

$$\nu_K \approx 0.27 Z\lambda \qquad \nu_M \approx 0.22\sigma_c Z\lambda$$

Modeling NL terms

$$\frac{\partial \mathbf{z}_\pm}{\partial t} = -\mathbf{z}_\mp\cdot\nabla\mathbf{z}_\pm$$

$$\frac{\partial}{\partial t}\langle z_+^2\rangle = -2\langle \mathbf{z}_+\cdot(\mathbf{z}_-\cdot\nabla\mathbf{z}_+)\rangle$$

$$\sim -\langle z_+^2\rangle\frac{\langle z_-^2\rangle^{-1/2}}{\lambda_+},$$

$$\frac{\partial Z^2}{\partial t} \sim -\frac{Z^3}{\lambda}$$

Usmanov et al., 2018

Boundary/Initial conditions and parameters (extra slide)

Symbol	Description	Value
N_0	proton number density in the initial state at 1 $R_\odot$	$8 \times 10^7\,\mathrm{cm}^{-3}$
T_0	electron and proton temperature in the initial state at 1 $R_\odot$	$1.8 \times 10^6\,\mathrm{K}$
B_0	magnetic field strength of dipole at 1 $R_\odot$	12 G
δv_0	driving amplitude of fluctuations in the initial state at 1 $R_\odot$	$35\,\mathrm{km\,s^{-1}}$
σ_{c0}	normalized cross helicity in the initial state	0.8
λ_0	correlation scale of turbulence in the initial state at at 1 $R_\odot$	0.015 $R_\odot$

Symbol	Description	Value
σ_D	normalized energy difference (residual energy)	$-1/3$
γ	adiabatic index	$5/3$
α_H	constant in Hollweg's collisionless heat flux	1.05
α, β	Kármán–Taylor constants	2, 0.128
f_p	fraction of turbulent heating for protons	0.6
r_H	collisional/collisionless electron heat flux transition region	5 $R_\odot$

Usmanov et al., 2018

Sample Results – Meridonal planes (30 Rs to 5 AU) and Comparison with Ulysses Data

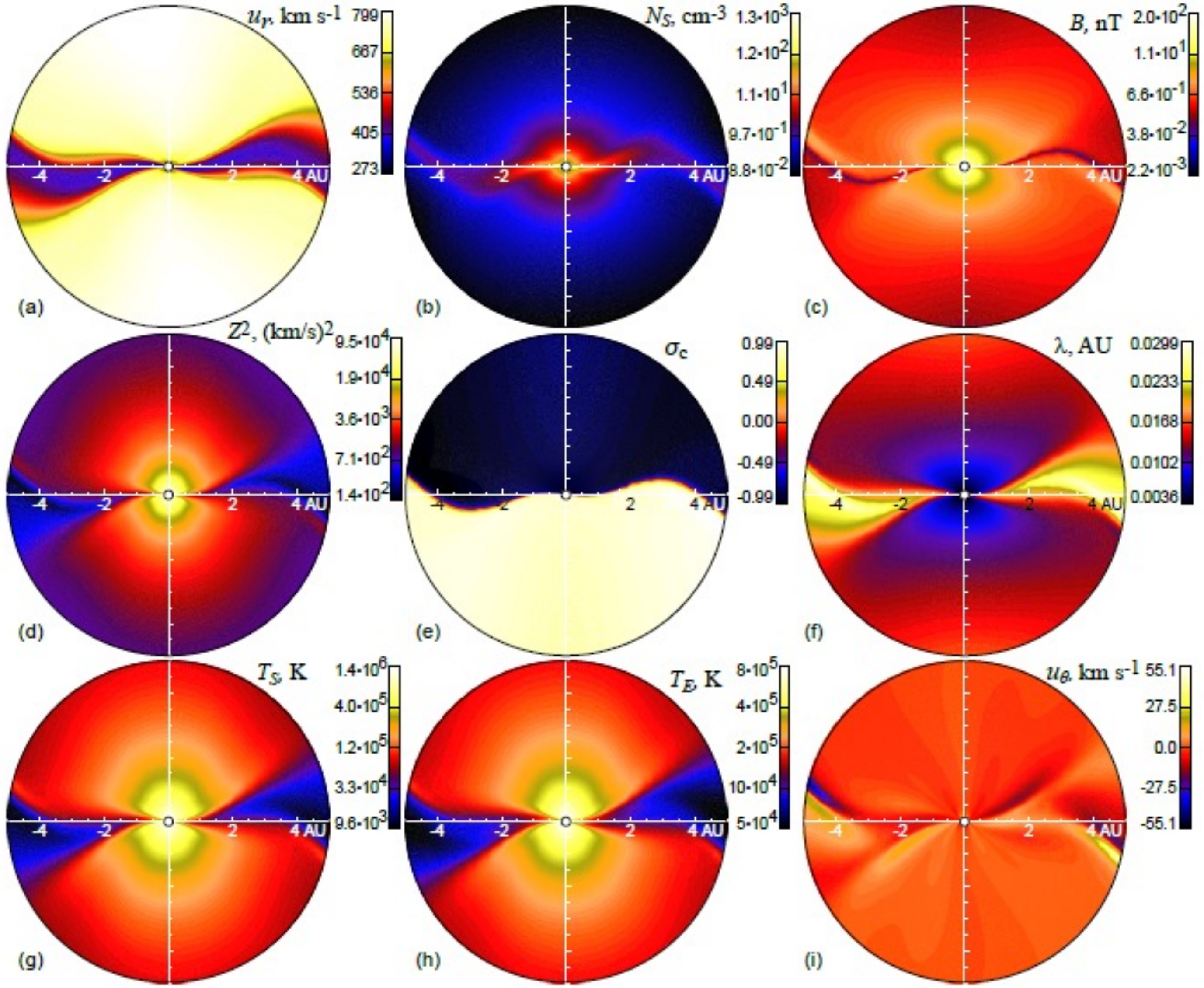

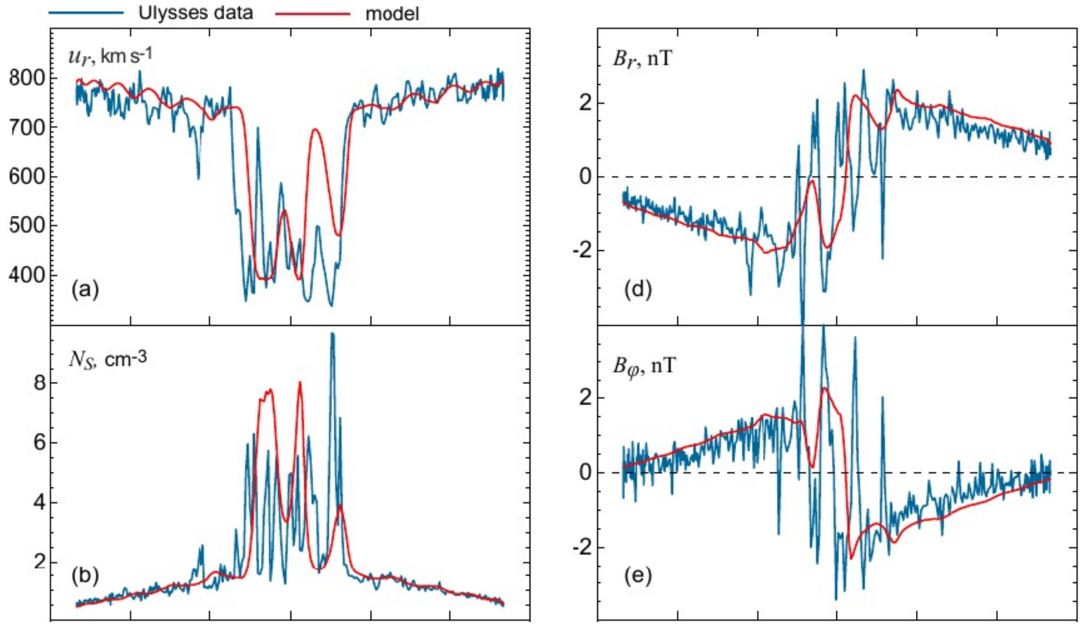

Usmanov et al., 2018

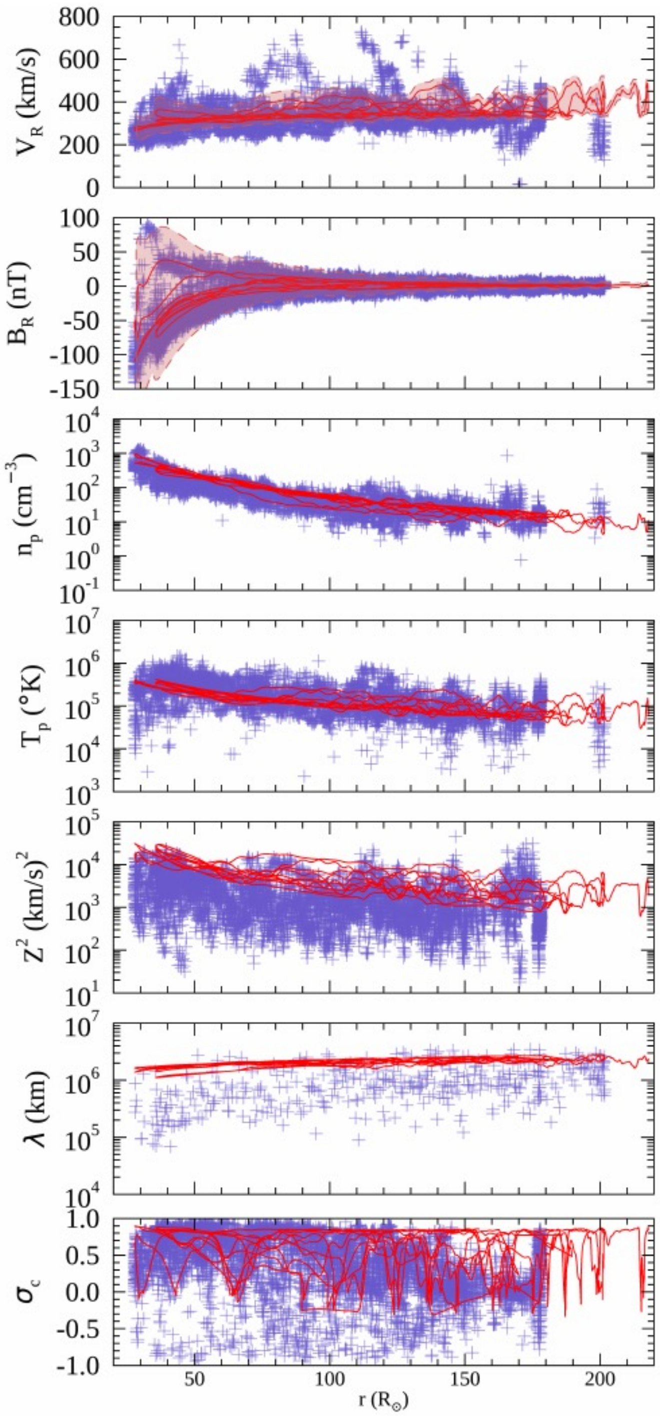

Radial trends aggregrated from first five PSP orbits

- Left: PSP data (symbols) aggregated from Orbits 1 to 5. Red curves show results from model, accumulated from five runs corresponding to the five respective orbits.
- Right: Mean values within bins of 10 solar radii from PSP data (blue circles) and model (red diamonds). Bars above and below symbols represent standard deviation.
- Averages reveal that radial trends in mean flow are quite well captured by the model (regardless of transient features seen in time series plots)
- Broad trends in turbulence properties also reproduced